

**LUMINESCENCE AND DEFECTS
CREATION PROCESSES
IN LEAD TUNGSTATE CRYSTALS**

ALEKSEI KRASNIKOV



TARTU UNIVERSITY
PRESS

The study was carried out at the Institute of Physics, University of Tartu.

The Dissertation was admitted on June 29, 2007 in partial fulfilment of the requirements for the degree of Doctor of Philosophy in physics (solid state physics), and allowed for defence by the Council of the Department of Physics, University of Tartu.

Supervisor: Dr. Svetlana Zazubovich, Institute of Physics, University of Tartu, Estonia

Opponents: Dr. Vladimir Makhov, Lebedev Physical Institute, Moscow, Russia

Dr. Larissa Grigorjeva, Institute of Solid State Physics, University of Latvia, Riga, Latvia

Defence: October 3, 2007, at University of Tartu, Tartu, Estonia

ISSN 1406-0647

ISBN 978-9949-11-695-9 (trükis)

ISBN 978-9949-11-696-6 (PDF)

Autoriõigus Aleksei Krasnikov, 2007

Tartu Ülikooli Kirjastus

www.tyk.ee

Tellimuse nr 317

CONTENTS

LIST OF PUBLICATIONS.....	6
I. INTRODUCTION.....	10
II. GENERAL BACKGROUND.....	12
1. Tungstate crystals.....	12
2. Crystal structure of tungstates.....	13
3. Electronic structure of PbWO_4	14
4. Scintillation characteristics of PbWO_4	15
III. EXPERIMENTAL.....	17
IV. PHOTOLUMINESCENCE CHARACTERISTICS OF PbWO_4 CRYSTALS.....	20
1. The blue (B) emission.....	20
2. The green (G) emission.....	23
3. The red (R) emission.....	28
V. PHOTO-THERMALLY STIMULATED DECAY OF THE EXCITON- AND DEFECT-RELATED STATES.....	32
1. Characteristics of thermally stimulated luminescence.....	32
2. Creation of electron and hole centers under irradiation in the exciton region.....	36
3. Creation of electron and hole centers under irradiation in the defect-related region.....	38
SUMMARY.....	40
SUMMARY IN ESTONIAN.....	42
REFERENCES.....	44
ACKNOWLEDGEMENTS.....	49
PUBLICATIONS.....	51

LIST OF PUBLICATIONS

This thesis is based on the following papers:

- I. E. Mihokova, M. Nikl, P. Bohacek, V. Babin, **A. Krasnikov**, A. Stolovich, S. Zazubovich, A. Vedda, M. Martini, T. Grabowski, “Decay kinetics of the green emission in $\text{PbWO}_4:\text{Mo}$ ”, *J. Lumin.*, vol. **102–103**, 618–622 (2003).
- II. M. Nikl, P. Bohacek, E. Mihokova, V. Babin, A. Stolovits, **A. Krasnikov**, S. Zazubovich, G. P. Pazzi, P. Fabeni, A. Vedda, M. Martini, “Excited state dynamics of luminescence centres in PbWO_4 single crystals”, *Functional Materials*, vol. **10**, 105–110 (2003).
- III. V. Babin, P. Bohacek, E. Bender, **A. Krasnikov**, E. Mihokova, M. Nikl, N. Senguttuvan, A. Stolovits, Y. Usuki, S. Zazubovich, “Decay kinetics of the green emission in tungstates and molybdates”, *Rad. Meas.*, vol. **38**, 533–537 (2004).
- IV. P. Bohacek, N. Senguttuvan, V. Kiisk, **A. Krasnikov**, M. Nikl, I. Sildos, Y. Usuki and S. Zazubovich, “Red emission of PbWO_4 crystals”, *Rad. Meas.*, vol. **38**, 623–626 (2004).
- V. P. Bohacek, P. Fabeni, **A. Krasnikov**, M. Nikl, G. P. Pazzi, C. Susini, S. Zazubovich, “Defects in UV-irradiated $\text{PbWO}_4:\text{Mo}$ crystals monitored by TSL measurements”, *Phys. Stat. Sol. (c)*, **2**, No.1, 547–550 (2005).
- VI. **A. Krasnikov**, M. Nikl, A. Stolovits, Y. Usuki, S. Zazubovich, “Luminescence of the $\text{PbWO}_4:5\% \text{ Cd}$ crystal”, *Phys. Stat. Sol. (c)* **2**, No.1, 77–80 (2005).
- VII. P. Bohacek, P. Fabeni, **A. Krasnikov**, M. Nikl, G. P. Pazzi, C. Susini, S. Zazubovich, “Defects creation under UV irradiation of PbWO_4 crystals”, *Radiation Protection Dosimetry*, **119**, No.1–4, 164–167 (2006).
- VIII. **A. Krasnikov**, M. Nikl, S. Zazubovich, “Localized excitons and defects in PbWO_4 single crystals: a luminescence and photo-thermally stimulated disintegration study” *Phys. Stat. Sol. (b)*, **243**, No. 8, 1727–1743 (2006).
- IX. **A. Krasnikov**, M. Nikl, S. Zazubovich, “Processes resulting in thermal quenching of the blue emission in PbWO_4 crystals”, *Proceedings of the Eighth Int. Conf. on Inorganic Scintillators and Their Applications (SCINT'2005)*, Eds. A. Gektin, B. Grinyov (Alushta, Ukraine, 2006) p. 362–365.

- X. P. Fabeni, V. Kiisk, **A. Krasnikov**, M. Nikl, G. P. Pazzi, I. Sildos, and S. Zazubovich, “Tunneling recombination processes in PbWO₄”, *Phys. Stat. Sol. (c)*, vol. **4**, pp. 918–921 (2007).
- XI. V. Babin, P. Bohachek, **A. Krasnikov**, M. Nikl, A. Stolovits, S. Zazubovich “Origin of green luminescence in PbWO₄ crystals”, *J. Lumin.*, vol. **124**, 113–119 (2007).
- XII. P. Fabeni, **A. Krasnikov**, V. V. Laguta, M. Nikl, G. P. Pazzi, C. Susini, and S. Zazubovich, “Origin of TSL peaks located at 200–250 K in UV-irradiated PbWO₄ crystals”, *Rad. Measur.*, vol. **42**, 807–810 (2007).
- XIII. **A. Krasnikov**, V. V. Laguta, M. Nikl, and S. Zazubovich, “Localized excitons and their decay into electron and hole centers in the PbWO₄ single crystals grown by the Bridgman method”, *J. Phys.: Condens. Matter* 2007, to be published.

The following papers are not related to the subject of the thesis:

- XIV. M. Nikl, J. A. Mares, E. Mihokova, K. Nitsch, N. Solovieva, V. Babin, **A. Krasnikov**, S. Zazubovich, M. Martini, A. Vedda, P. Fabeni, G. P. Pazzi, S. Baccaro, “Radio- and thermoluminescence and energy transfer processes in Ce³⁺(Tb³⁺)-doped phosphate scintillating glasses”, *Rad. Meas.*, vol. **33**, 593–596 (2001).
- XV. V. Babin, K. Kalder, **A. Krasnikov**, S. Zazubovich, “Luminescence and defects creation under photoexcitation of CsI:Tl crystal in Tl⁺-related absorption bands”, *J. Lumin.*, vol. **96**, 75–85 (2002).
- XVI. V. Babin, K. Kalder, **A. Krasnikov**, M. Nikl, K. Nitsch, S. Zazubovich, “Defects creation under UV irradiation of CsI:Pb crystals in Pb²⁺-induced absorption bands investigated by luminescence methods”, *Phys. Stat. Sol. (b)*, vol. **234**, 689–700 (2002).
- XVII. V. Babin, **A. Krasnikov**, H. Wiczorek, S. Zazubovich, “Luminescence of complicated thallium centres in CsI:Tl”, *Nuclear Instr. & Meth. A*, vol. **486**, 486–489 (2002).
- XVIII. M. Nikl, J. A. Mareš, J. Chval, E. Mihokova, N. Solovieva, M. Martini, A. Vedda, K. Blazek, P. Maly, K. Nejezchleb, P. Fabeni, G. P. Pazzi, V. Babin, K. Kalder, **A. Krasnikov**, S. Zazubovich, C. D’Ambrosio, “An effect of Zr⁴⁺ co-doping of YAP:Ce scintillator”, *Nuclear Instr. & Meth. A*, vol. **486**, 250–253 (2002).

- XIX. V. Babin, **A. Krasnikov**, M. Nikl, A. Stolovits, S. Zazubovich, “On interpretation of luminescence of lead halide crystals”, *Phys. Stat. Sol. (b)*, vol. **229**, 1295–1304 (2002).
- XX. J. A. Mares, M. Nikl, K. Nitsch, N. Solovieva, **A. Krasnikov**, S. Zazubovich, “A role of Gd^{3+} in Tb-doped Na-Gd phosphate glasses”, *J. Lumin.*, vol. **94–95**, 321–324 (2001).
- XXI. V. Babin, **A. Krasnikov**, S. Zazubovich, “Charge-transfer processes in doped alkali halides”, *Rad. Eff. & Def. Solids*, vol. **158**, 227–230 (2003).
- XXII. V. Babin, **A. Krasnikov**, J. A. Mares, M. Nikl, K. Nitsch, N. Solovieva, S. Zazubovich, “Luminescence spectroscopy of the Gd-rich Ce^{3+} , Tb^{3+} - and Mn^{2+} -doped phosphate glasses”, *Phys. Stat. Sol. (b)*, vol. **196**, 484–495 (2003).
- XXIII. V. Babin, **A. Krasnikov**, M. Nikl, K. Nitsch, A. Stolovits, S. Zazubovich, “Luminescence and relaxed excited state origin in CsI:Pb crystals”, *J. Lumin.*, vol. **101**, 219–226 (2003).
- XXIV. P. Fabeni, **A. Krasnikov**, M. Nikl, G. P. Pazzi, S. Zazubovich, “Stimulated self-trapped exciton emission in CsI:Pb”, *Solid State Commun.*, vol. **126**, 665–669 (2003).
- XXV. K. Blazek, **A. Krasnikov**, K. Nejezchleb, M. Nikl, T. Savikhina, S. Zazubovich, “Luminescence and defects creation in Ce^{3+} -doped $Lu_3Al_5O_{12}$ crystal”, *Phys. Stat. Sol. (b)*, vol. **241**, 1134–1140 (2004).
- XXVI. D. Dimartino, **A. Krasnikov**, M. Nikl, A. Vedda, S. Zazubovich, “The 3.83 eV luminescence of Gd-enriched phosphate glasses”, *Phys. Stat. Sol. (a)*, vol. **201**, R38–R40 (2004).
- XXVII. **A. Krasnikov**, T. Savikhina, S. Zazubovich, M. Nikl, J. A. Mares, K. Blazek, K. Nejezchleb, “Luminescence and defects creation in Ce^{3+} -doped aluminium and lutetium perovskites and garnets”, *Nucl. Instr. & Meth. Phys. Res. A* **537** 130–133 (2005).
- XXVIII. V. Babin, **A. Krasnikov**, M. Nikl, T. Savikhina, S. Zazubovich, “Luminescence of undoped LuAG and YAG crystals”, *Phys. Stat. Sol. (c)*, **2**, No. 1, 97–100 (2005).
- XXIX. M. Nikl, H. Ogino, **A. Krasnikov**, A. Beitlerova, A. Yoshikawa and T. Fukuda “Photo- and radioluminescence of Pr-doped $Lu_3Al_5O_{12}$ single crystal”, *Phys. Stat. Sol. (a)* **202**, No. 1, R4–R6 (2005).
- XXX. K. Blazek, **A. Krasnikov**, K. Nejezchleb, M. Nikl, T. Savikhina, S. Zazubovich, “Luminescence and defects creation in Ce^{3+} -doped

YAlO₃ and LuYAlO₃ crystals”, *Phys. Stat. Sol. (b)*, **242**, No. 6, 1315–1323 (2005).

- XXXI. H. Ogino, A. Yoshikawa, M. Nikl, **A. Krasnikov**, K. Kamada, T. Fukuda, “Growth and Scintillation properties of Pr doped Lu₃Al₅O₁₂ crystals”, *Journal of Crystal Growth*, vol. **287**, 335–338 (2006).
- XXXII. M. Nikl, K. Kamada, A. Yoshikawa, **A. Krasnikov**, A. Beitlerova, N. Solovieva, J. Hybler, T. Fukuda, “Luminescence characteristics and energy transfer in the mixed Y_xGd_{1-x}F₃:Ce, Me (Me = Mg, Ca, Sr, Ba) crystals”, *J. Phys.: Condensed Matter*, vol. **18**, 3069–3079 (2006).
- XXXIII. V. Babin, P. Fabeni, **A. Krasnikov**, K. Nejezchleb, M. Nikl, G. P. Pazzi, T. Savikhina, S. Zazubovich, “Irregular Ce³⁺ and defect-related luminescence in YAlO₃ single crystal”, *J. Lumin.*, vol. **124**, 273–278 (2007)
- XXXIV. V. Babin, **A. Krasnikov**, Y. Maksimov, K. Nejezchleb, M. Nikl, T. Savikhina, S. Zazubovich, “Luminescence of Pr³⁺-doped garnet single crystal”, *Optic. Mater.*, vol. **30**, 30–32 (2007).
- XXXV. M. Nikl, H. Ogino, **A. Krasnikov**, E. Mihokova, J. Pejchal, A. Yoshikawa, A. Vedda, M. Fasoli, T. Fukuda, “Charge transfer luminescence in Yb³⁺-doped Lu₃Al₅O₁₂ single crystal”, *J. Phys.: Condens. Matter*, submitted.

I. INTRODUCTION

The scintillation method is widely used for detection of various kinds of ionizing radiation. A scintillator is a material able to convert energy of absorbed high energy photon or particle (electron, proton, neutron, α -particle, etc.) into a number of UV or visible photons. These emitted photons are detectable with photomultiplier tube or photodiode required to convert the light into an electrical pulse.

Scintillation detectors, transforming the ionizing radiation into visible light, are widely used in medicine (X-ray computed tomography, positron emission tomography, mammography used, e.g. in cancer diagnostics, brain mapping, optimization of drug dosage and its circulation in human body), where better medical diagnostics is immediately reflected in better quality of medical care and in improved general health of human population. They are widely used in security systems (becoming increasingly important in customs checking in airports and at the borders), environmental monitoring, geology, space investigations, industrial defectoscopy, radiation protection, electron microscopy, accelerators for high-energy physics experiments, etc.

The progress in the high-energy physics and nuclear physics stimulated research in scintillation materials science. This is the search and development of new perspective materials for scintillators and further improvement of the traditional scintillators. The development was prompted by requirements of new and existing applications in many fields of human activity, which use ionising radiation.

Single crystals of lead tungstate (PbWO_4) became a subject of renewed interest about 15 years ago when their favourable characteristics for scintillation detection were reported [1, 2]. Low production costs and high density could make lead tungstate a serious competitor of the materials currently used in the field of industrial or even medical applications. Because of potential application of lead tungstate crystals in electromagnetic calorimeters – the inner parts of detectors used in accelerators for high energy physics experiments, a huge amount of papers appeared since this time, which were devoted to the study of their luminescence characteristics, energy storage and transfer processes, radiation damage, etc. (see, e.g., reviews [3–5]). However, despite the intense studies, the origin of luminescence centers and traps for electrons and holes, and the processes of creation and recombination of various electron and hole centers are still under discussion.

Therefore the main purposes of the present work were the following:

- The detailed study of characteristics of photo- and thermoluminescence, the clarification of the origin of luminescence centers and mechanisms of luminescence.

- The explanation of photo-thermally stimulated processes of various exciton and defect-related states disintegration.
- The explanation of origin of various optically created electron and hole centers and their role in recombination and scintillation processes.
- Also, one of the goals of our experimental work was to give the necessary information to developers of scintillation materials for determination of the conditions (e.g., host material composition, doping and codoping ion type and optimum concentration, procedure of preparation and subsequent thermal treatment) which allows to achieve the needed scintillation characteristics (e.g., high light yield, fast luminescence decay, good energy and spatial resolution, high stability, etc).

In the present work, a review of our results [6–14] obtained at systematic study of the luminescence and photo-thermally stimulated defects creation processes, occurring under selective UV irradiation, is presented. Dependences of the number of optically created electron and hole centers on the irradiation energy, irradiation temperature and irradiation duration were measured under irradiation of a crystal in the band-to-band, exciton and defect-related absorption regions. The optically created centers were detected by the TSL and ESR methods. The data obtained at the investigation of more than thirty various undoped and doped PbWO_4 crystals, containing different concentrations of various impurity and crystal structure defects, grown by different methods, in different laboratories, and annealed at different conditions were compared.

II. GENERAL BACKGROUND

1. Tungstate crystals

Crystals on the basis of tungsten compound retain attention of researchers already for a long time and have found wide application as scintillators and luminophors.

The tungstate structural type shares between two groups: sheelite (CaWO_4 , BaWO_4 , SrWO_4 and PbWO_4) and wolframite (MgWO_4 , ZnWO_4 , CdWO_4 , etc.). Tungstates of the wolframite structural type possess an intense luminescence in visible area of a spectrum. Magnesium tungstate is used as photoluminophor already for a long time [15], and cadmium and zinc tungstates are known as perspective materials for scintillation detectors in the field of a computer tomography [16].

Tungstates of the sheelite structural type, despite of identical crystal structure, possess noticeably different luminescent properties defining an opportunity of their practical application.

Calcium tungstate is an effective x-ray luminophor, which is used already more than hundred years in medical screens and luminescent lamps. Its advantages are an intense luminescence in visible area of a spectrum and a high constant light yield. However, a minus of this compound is a slow luminescence decay (decay time about $100 \mu\text{s}$) that leads to impossibility of work with intense streams of quanta (more than 10^6 photons/sec) and also its uses in the devices demanding the time resolution.

Last years the big interest involves one more crystal with sheelite structure – lead tungstate – PbWO_4 [17–19]. Despite of the smallest light yield of 50 photons/MeV (that corresponds to energy output in hundreds times smaller, than at CaWO_4), lead tungstate possesses high density, radiation stability, and the main thing, short (ns) decay time of a luminescence at a room temperature. Owing to these properties, PbWO_4 is going to be used as scintillator for the experiments in high energy physics. In this case the requirement of a high light yield of a luminescence is not the core owing to high energy of registered particles (100 GeV).

Unlike the last two crystals, in barium tungstate the luminescence is absent at room temperatures. A weak luminescence is observed at helium temperatures that does not allow to use its luminescent properties.

It is obvious, that distinction of tungstate-sheelite luminescent properties is connected with different influence on these properties of cations, i.e. calcium, barium and lead.

2. Crystal structure of tungstates

Tungsten oxocations form with bivalent cations from the second and eighth groups of periodic system, and also with Mn, Pb a sequence of compounds with general formula ABO_4 , where A – Mg, Mn, Fe, Co, Ni, Zn, Cd, Ca, Sr, Ba, Pb; B – Mo, W. This sequence breaks up to group of tungstates of bivalent cations with $r < 0.1$ nm (r – the cation radius) for which the wolframite structural type is characteristic (monoclinic system, spatial group P2/c) and to group with cation radius $r > 0.1$ nm, with sheelite structural type (tetragonal system, spatial group C_{4h}^6 (I4₁/a)) [20]. Transition from wolframite structural type to sheelite type is on the border of cations Cd – Ca. However, the change of structural type cannot be explained only by the geometrical factor of increase in the cation radius. For example, Pb^{2+} has $r = 0.12$ nm, however $PbWO_4$ can crystallize both in sheelite structural type – β – $PbWO_4$, *shtolzit* (as $r > 0.1$ nm,) and in wolframite structural type – α – $PbWO_4$, *raspite* (on the basis of effect of polarization [21]).

The sheelite elementary unit cell consists of four molecules ABO_4 (Fig.1). The basis of sheelite structure consists of the three-dimensional carcass formed by infinite zigzag-like chains of polyhedrons of metal A^{2+} . Between two close polyhedrons, single, not connected with each other ortotetrahedrons BO_4^{2-} are located. In turn, each cation A^{2+} is surrounded by eight atoms of oxygen, which form the distorted octahedron with cation A^{2+} in the centre. The connection between cation A^{2+} and anion BO_4^{2-} is ionic, and connections B-O inside the oxianion complex in the sheelite structure is covalent. In Table 1, the characteristic crystal parameters of ABO_4 crystals with sheelite and wolframite structure, received by means of x-ray and neutron diffraction, are presented.

In work [20] it is noted, that the wolframite – sheelite transformation is not sharply expressed: the wolframite structure can be considered as the distorted sheelite structure. However, the presence of isolated oxianion complexes is the most important difference of the sheelite structure from the wolframite structure.

Further only one tungstate with sheelite structure – lead tungstate crystal ($PbWO_4$) will be considered.

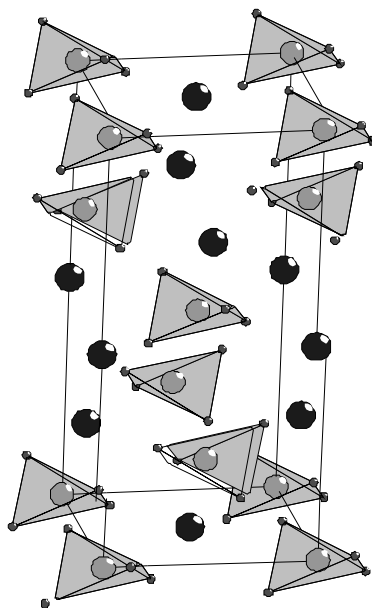


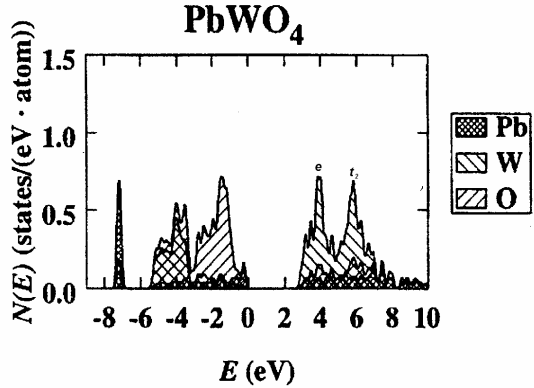
FIG. 1. Atoms in a tetragonal unit cell of sheelite. Atoms of tungsten are inside in tetrahedrons in which tops atoms of oxygen are located. Cation atoms – big spheres outside of tetrahedrons.

Table 1. Unit-cell parameters (in angstroms) of some ABO₄ crystals [5, 20].

Crystal	Spatial group	Cation radius A ²⁺ , 10 ⁻¹⁰ M	Unit-cell parameters			
			a	b	c	β
MgWO ₄	P2/c	0.66	4.69	5.68	4.92	89°40′
ZnWO ₄	P2/c	0.74	4.68	5.73	4.95	89°30′
CdWO ₄	P2/c	0.97	5.02	5.85	5.07	91°29′
CaWO ₄	I4 ₁ /a	0.99	5.242		11.372	
PbMoO ₄	I4 ₁ /a	1.2	5.47		12.18	
PbWO ₄	I4 ₁ /a	1.2	5.462		12.046	
PbWO ₄	P2/c	1.2	5.58	5.00	13.64	107°33′

3. Electronic structure of PbWO₄

Energy-band structure of PbWO₄ sheelite was calculated by cluster method of molecular orbitals and a method of linearized-augmented-plane-wave (LAPW) [22–25]. Both methods gave close results on interposition of electronic terms in a valence band (VB) and in a conductivity band (CB). The basic contribution to top of VB is brought with states O 2*p*, and to bottom of CB, with states W 5*d*. The degenerated W 5*d* states are split in a crystal field of tetragonal symmetry on *e*- and *t*₂-terms. In PbWO₄ sheelite structure, the *e*-terms are the lower, and the *t*₂-terms, the higher ones (Fig. 2). Contribution of Pb in CB is mainly defined by 6*p*-states.

**FIG. 2.** Partial density of states defining contribution of Pb, W and O, for VB and CB of PbWO₄ crystal with sheelite structure [23].

Thus, at the excitation of sheelite crystals in the region of fundamental absorption, the electronic transitions with charge transfer of two types can be observed: (i) within the molecular anion, i.e. from oxygen to tungsten, or (ii) from oxygen to a lead ion.

Due to noticeable contribution of Pb 6*s* states in the top of VB of PbWO₄, the role of cation excitation in optical characteristics of this crystal can be considerable. In Fig. 3, the schematic diagram of a crystal field splitting and hybridization of the molecular orbitals of an oxianion tetrahedral complex of PbWO₄ crystal is presented.

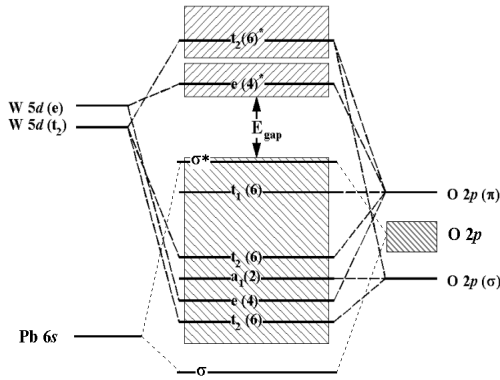


FIG. 3. The schematic diagram of molecular orbitals for transitions W-O and Pb-O is imposed on the shaded areas representing VB and CB, calculated for crystal PbWO_4 [24].

4. Scintillation characteristics of PbWO_4

The scintillating PbWO_4 crystals have a number of excellent properties compared with other well-known inorganic crystal scintillators such as NaI:Tl and $\text{Bi}_4\text{Ge}_3\text{O}_{12}$ [1, 2, 26]. Some characteristics of practically important and/or intensively researched scintillation materials are given in Table 2. PbWO_4 is the most attractive for high-energy physics applications because of its high density (8.23 g/cm^3), short decay time (less than 10 ns for major part of the light output) and high radiation damage resistance (10^6 rad for undoped and 10^8 rad for La-doped PbWO_4) [28, 29]. But serious drawback of this scintillator is its low light yield (about 2–3% with respect to $\text{Bi}_4\text{Ge}_3\text{O}_{12}$). Some research laboratories tried to increase the light yield of PWO by a suitable doping [30, 31]. For example, double doping by Mo^{6+} and A^{3+} ($\text{A}=\text{La}, \text{Y}$) ions appeared as the most successful way, providing a light yield increase by a factor of 2–3 [31, 32] without the deterioration of other scintillation characteristics. Codoping with trivalent ions increases also the speed of photoluminescence and scintillation response [3, 5] by removing the slow (μs -s) decay components. A favorable influence of trivalent ion codoping was evidenced also in a lower concentration of trapping states and higher radiation hardness with respect to undoped PbWO_4 and $\text{PbWO}_4:\text{Mo}$ [32–34]. Thus, doping allows to improve scintillation properties of the lead tungstate crystal.

Table 2. A survey of characteristics of selected single crystal scintillators [27].

Crystal	Density (g cm ⁻³)	Light yield (photon MeV ⁻¹)	Dominant scintillation decay time (ns)	Emission maximum (nm)
CsI:Tl	4.51	66000	800	550
NaI:Tl	3.67	41000	230	410
LaBr ₃ :Ce	5.3	61000	35	358
K ₂ LaI ₅ :Ce	4.4	55000	24	420
BaF ₂ (only cross luminescence)	4.88	1500	0.6–0.8	180–220
Bi ₄ Ge ₃ O ₁₂	7.1	8600	300	480
PbWO ₄	8.28	300	2–3	410
CdWO ₄	7.9	20000	5000	495
YAlO ₃ :Ce	5.6	21000	20–30	360
LuAlO ₃ :Ce	8.34	12000	18	365
Y ₃ Al ₅ O ₁₂ :Ce	4.56	24000	90–120	550
Lu ₃ Al ₅ O ₁₂ :Ce	6.67	12500	55	530
Gd ₂ SiO ₅ :Ce	6.7	8000	60	420
Lu ₂ SiO ₅ :Ce	7.4	26000	30	390

A brief review of the works devoted to the study of luminescence characteristics of PbWO₄ crystals will be given in the corresponding chapters of the thesis.

III. EXPERIMENTAL

The undoped and doped PbWO_4 crystals prepared in Czech Republic and in Japan by the Czochralski or Bridgman methods, as-grown or annealed at different conditions, containing strongly different concentrations of impurity ions and crystal structure defects (for more details, see corresponding author's publications [6–8, 11, 12]) were studied in a wide temperature range by the methods of steady-state and time-resolved luminescence spectroscopy and also by the thermally stimulated luminescence (TSL) and electron spin resonance (ESR) methods.

The experiments were carried out in different laboratories.

In *Tartu laboratories*, the steady-state *emission and excitation spectra* were measured with the use of the following set-up (for more details see [35] and references therein). The luminescence characteristics were studied on excitation by deuterium (DDS-400) or mercury (SVD-120) lamps through the monochromator (prism SF-4 or grating MDR-2). The emission was selected by another prism monochromator (SPM-1) or a system of optical filters and detected by a photomultiplier tube (FEU-39, FEU-79, FEU-83). Additionally, another experimental set-up, created by the author, was used. It consists of xenon (ORIEL Xe, 150W) lamp, two monochromators (grating MDR-3 and ORIEL Cornerstone) and photon counting head (Hamamatsu). This experimental set-up was controlled with computer via GPIB PC-card. Necessary software was created with the use of the LabView developed environment 8.0.

The *time-resolved experiments* were carried out using analogous set-up's. The luminescence was excited by xenon flashlamp FX-1152 (EG&G) with pulse duration 700 ns. The luminescence was detected by the photomultiplier and registered by PC multichannel scaler MCS-plus (EG&G) with time resolution 2 μs . The start of the scan was synchronized with the start of the flashlamp arc discharge. All the scans were repetitive, multiple scans were summed to diminish the statistical scatter in the recorded pattern. Parameters of decay curves were determined by means of program *Spectra* using standard procedures of the least square method. Experimental decay curves are usually non-elementary and consequently the program makes their decomposition on separate exponential components by approximation with simple set of exponents. If the decay curve consists of several components whose decay time differs less than in 1.5 times, its exact decomposition appears impossible. The decay time τ of each luminescence decay component was determined as a time interval in which the intensity of its component decreases by e times. The light sum of the component was determined as $I_0 \cdot \tau$, where I_0 is the number of pulses in the first channel of the analyzer and τ is the decay time of the component expressed in the quantity of channels.

Thermally stimulated luminescence glow curves $I_{\text{TSL}}(T)$ were measured with a constant heating rate of 0.2 K/s for the crystal, preliminarily UV irradiated by the deuterium DDS-400 lamp through the monochromator SF-4 (with spectral widths of the slit 2–5 nm). The TSL intensity was detected by FEU-39 or FEU-79. The dependences of maximum intensities of the TSL peaks (I_{TSL}) on the irradiation energy (E_{irr}) (TSL peak creation spectra) were measured for all the TSL peaks after irradiation of the crystal at different temperatures (T_{irr}). The TSL intensity dependences on the irradiation temperature were measured under irradiation with different irradiation energies to obtain the activation energies (E_a) for different TSL peaks' creation. To avoid the irradiation-induced destruction of the centers responsible for the TSL peak studied, the irradiation temperature was at least 50 K smaller than the temperature of the TSL peak maximum.

The sample was placed into a vacuum nitrogen cryostat (down to 77 K), immersion helium cryostat (down to 1.7 K) or special helium cryostat. The last one allowed us to obtain temperatures down to 0.35 K by pumping out the ^3He vapour.

A block diagram of a commonly used experimental set-up is presented in Fig. 4.

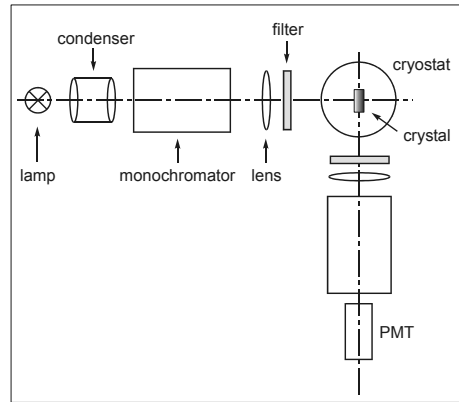


FIG. 4. The scheme of experimental set-up.

In *Prague laboratory* (Institute of Physics, AS of Czech Republic), the steady-state and time-resolved emission spectra and decay kinetics in the ns-ms time scale were measured using spectrofluorometer 199S (Edinburgh Instruments) modified for low temperature measurements (4.2–300 K). In single photon counting method, the excitation by a nanosecond coaxial flashlamp filled with hydrogen (the full width at a half maximum (FWHM) of excitation pulse about 1.5 ns) or alternatively by a FX108AU xenon microsecond pulse flashlamp and multichannel analyser in the scanning mode, was used for decay kinetics measurements in the ns and μs -ms time scale, respectively (for more details see, e.g. [36]).

The ESR measurements were performed at 9.21 GHz in the standard 3 cm wavelength range of an ESR spectrometer at temperatures of 4–300 K. An Oxford Instruments ESR-9 cryosystem was used. The applied magnetic field was rotated in the (001) and (100) planes of the PWO crystal structure. A mercury high pressure arc lamp and a halogen tungsten lamp with both broad and narrow bandpass optical filters were used for spectrally resolved optical irradiation of the samples [37].

In *Florence laboratory* (Institute of Applied Physics, CNR, Italy), the decay kinetics in ns-ms time scale and emission spectra in the 300–800 nm spectral range at 10–300 K (closed cycle helium refrigerator Galileo K1C-ST) were measured under the excimer XeCl (4.02 eV) or nitrogen (3.677 eV) laser excitation. The luminescence was measured with the monochromator Triax 320 (Jobin-Yvon) and detected by a photomultiplier coupled with a digital Tektronix TDS-680B sampling oscilloscope or by the OMA (EG&G PARC) detector head, respectively. This setup is described in more detail in [38].

Thermally stimulated luminescence glow curves were measured after irradiation of a crystal, located inside a close-cycle refrigerator, at 80–180 K for 15 or 30 min in the 3.4–4.3 eV energy range with a xenon 150 W lamp through a monochromator with 1.0 mm slits (spectral width 6 nm). The TSL intensity was detected through an Oriel 500 nm filter by a photomultiplier whose output was sent through an amplifier/inverter to an A/D card inserted in a PC. The setup allowed to detect the TSL intensity in an amplitude range of 3–4 orders of magnitude. The crystal heating rate was 0.18 ± 0.02 K/sec. The TSL intensity (I_{TSL}) dependences on the irradiation energy (E_{irr}) and irradiation temperature (T_{irr}) were measured.

All spectra were corrected for the spectral distribution of the exciting light, transmission of cryostat windows and monochromators, dispersion of monochromators, and the spectral sensitivity of detectors.

IV. PHOTOLUMINESCENCE CHARACTERISTICS OF PbWO₄ CRYSTALS

In the luminescence spectrum of PbWO₄ crystals, several emission bands located in the blue, green and red spectral regions are present (see, e.g., [5, 18, 34], [39–47], [49–66]). Their relative intensities depend strongly on the sample.

1. The blue emission

The so-called *blue (B) emission* (2.8–2.9 eV) was ascribed to the self-trapped exciton (STE) around the (WO₄)²⁻ molecular anion (see [47], [3–5] and references therein). In some papers [39–49] the decay kinetics of the B emission were measured. To describe temperature dependences of the B emission intensity $I(T)$ and decay time $\tau(T)$ by a phenomenological model (see Fig. 5, Table 3), two thermally stimulated processes were considered in [48]: the intracentre thermal quenching characterized by the activation energy $E_Q=0.2$ eV and frequency factor $w_Q=10^{12}$ s⁻¹, and the regular exciton disintegration with $E_{ED}=0.1$ eV and $w_{ED}=10^9$ s⁻¹.

In order to clarify the origin of the B emission and the processes, resulting in its thermal quenching, the emission and excitation spectra, temperature dependences of the emission intensity as well as the photo-thermally stimulated processes of the self-trapped and localized exciton states disintegration were studied by us.

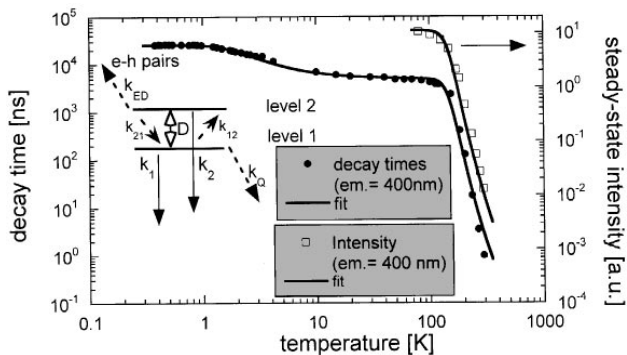


FIG. 5. Temperature dependence of the decay times and steady-state intensities related to the prompt part of the self-trapped exciton emission in PbWO₄. Solid lines come from the model sketched in the figure with the parameters summarized in Table 3. The parameters k_1 , k_2 stand for the radiative rates from the excited state levels 1 and 2, respectively, k_{12} and k_{21} are the nonradiative rates interconnecting the levels 1 and 2. Parameter D is the energy separation between the levels 1 and 2. Finally, k_Q stands for a nonradiative quenching rate and k_{ED} stands for a thermally induced exciton disintegration rate, where the latter is supposed to take place from the relaxed excited state. Both k_Q and k_{ED} are considered in a standard form $k_i = w_i \exp[-E_i/kT]$, where w_i and E_i stand for the frequency factor and activation energy, respectively (see also Ref. [48], [49]).

Table 3. Parameters (see also Fig. 5) of the relaxed excited states responsible for the blue(*) and green emission. Parameter K is a “zero temperature” rate related to k_{12} and k_{21} parameters (for more detail see [48], [67]).

Crystal	D, meV	k_1, s^{-1}	k_2, s^{-1}	K, s^{-1}	w_{ED}, s^{-1}	E_{ED}, eV
*PbWO ₄	0.45	3.9×10^4	3.7×10^5	5×10^5	1×10^9	0.1
PbWO ₄	0.3	4.05×10^3	1.0×10^5	0.6×10^5	1×10^8	0.1
PbWO ₄ :Cr	0.33	4.72×10^3	1.2×10^5	1.0×10^5	1×10^8	0.1
PbWO ₄ :Mo	0.35	4.1×10^3	8.3×10^4	3.0×10^5	7×10^{12}	0.26
PbMoO ₄	0.37	6.3×10^3	1.3×10^5	1.0×10^5	5×10^{13}	0.26
CdWO ₄	1.2	3.12×10^3	9.5×10^4	1.2×10^5	–	–
ZnWO ₄	1.0	4.98×10^3	5.8×10^4	1.0×10^5	7×10^8	0.29

Luminescence studies showed that the *B emission* spectrum (see e.g., Fig. 6) consists of strongly overlapping bands, arising from the self-trapped and localized excitons of the type of $(WO_4)^{2-}$ [11–13]. This is evident from (i) slightly different positions (2.72–2.78 eV) and halfwidths (FWHM=0.59–0.69 eV) of the B emission band and slightly different positions of the lowest-energy excitation band of the B emission in different crystals; (ii) the dependence of the B band position on excitation energy (Fig. 7) and the excitation spectrum of the B emission, on the emission energy (Fig. 8), observed in some crystals; (iii) different temperature dependences of the B emission intensity in different crystals (Fig. 9) (the temperature T_q , where the intensity decreases twice from its maximum value at $T < 80$ K, varies in different crystals from 147 K to 197 K).

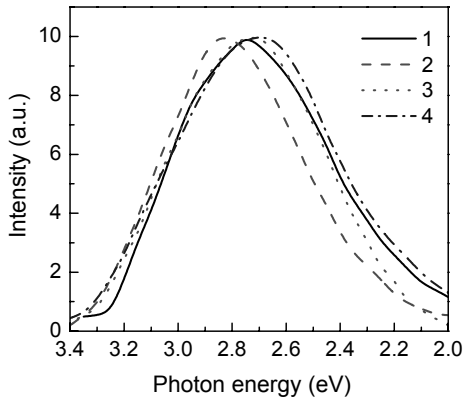


FIG. 6. Emission spectra measured at 4.2 K under the band-to-band excitation for three undoped PbWO₄ crystals: pwjp96 (1), pwjp99 (2) and pw154 (3), and for PbWO₄:50000 ppm Cd (4).

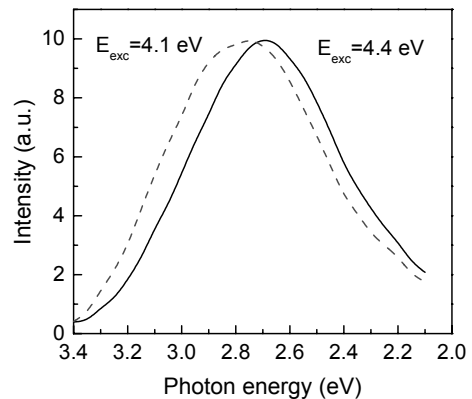


FIG. 7. Emission spectra of undoped as-grown PbWO₄ Bridgman crystal measured at 80 K under $E_{exc}=4.4$ eV and $E_{exc}=4.1$ eV.

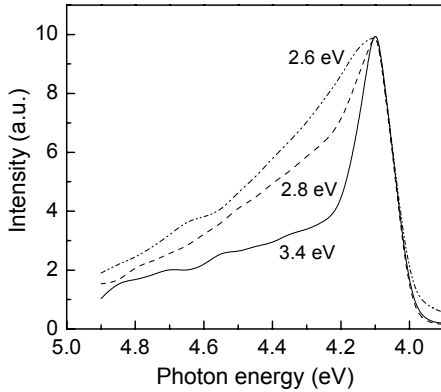


FIG. 8. Excitation spectra of the PbWO_4 as-grown Bridgman crystal measured at 80 K for $E_{\text{em}}=3.4$ eV, $E_{\text{em}}=2.8$ eV and $E_{\text{em}}=2.6$ eV.

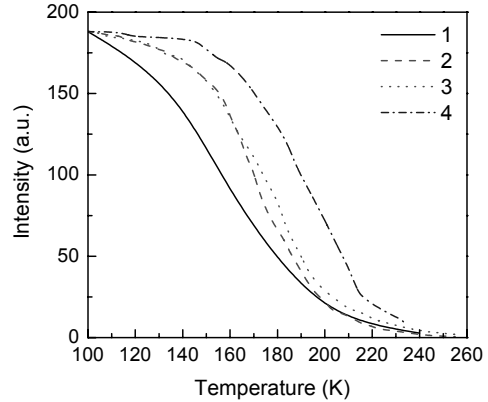


FIG. 9. Temperature dependences of the blue emission intensity measured under the band-to-band excitation for the undoped PbWO_4 crystals: pwjp96 (1), pwjp99 (2) and pw154 as-grown (3), and for the PbWO_4 :50000 ppm Cd crystal (4).

Our studies have shown that the mentioned effects do not arise from the overlap of the blue and green emission bands as they are independent of relative intensity of the green emission (the B/G emission intensity ratio, see Table 4).

From the $\ln I(1/T)$ dependences, the activation energy E_q of the emission thermal quenching was determined. It was found that thermal quenching of the B emission at $T > 180$ K takes place with the activation energy $E_q \approx 0.20$ eV. At $T < 160$ K, the B emission intensity decreases with $E_q \approx 0.08$ eV and $E_q < 0.04$ eV (Fig. 10). As it will be shown further (see Chapter V), the quenching with the mentioned E_q values can be explained by the decay of the localized excitons, self-trapped excitons and by the charge-transfer-processes in close defect pairs, respectively.

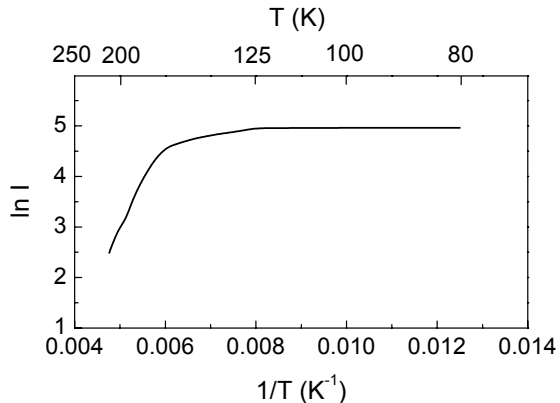


FIG. 10. The $\ln I(1/T)$ dependences obtained under $E_{\text{exc}}=4.4$ eV for the B emission of the PbWO_4 :Mo, Ce crystal.

Table 4. The B emission band maxima (E_m^I) and halfwidths (FWHM), the excitation band maxima ($E_{\text{exc}}^{\text{max}}$), and the B/G(I) emission intensity ratios obtained from the uncorrected spectra measured at 4.2 K (with FEU-79) for various PbWO_4 (PWO) crystals. The temperatures T_q where the emission intensity decreases twice from its value at $T < 80$ K.

Crystal	E_m^I , eV	FWHM, eV	$E_{\text{exc}}^{\text{max}}$, eV	T_q , K	B/G(I) ratio
<i>Mo-doped crystals</i>					
PWO:135 ppm Mo (Japan)	2.77	0.65	4.17	158	0.22
PWO:1000 ppm Mo	2.78	0.65	4.20	185	0.19
PWO:200 ppm Mo (87e)	2.66	0.68	4.16	161	0.13
PWO:200 ppm (95b)	2.78	0.65	4.17	181	0.20
PWO:200 ppm Mo/200 ppm Y	2.78	0.62	4.17	177	0.18
PWO:200 ppm Mo/100 ppm Nb	2.75	0.68	4.15	147	~0.08
PWO:800 ppm Mo/ 60 ppm Ce	2.76	0.615	4.17	176	0.40
<i>Undoped crystals</i>					
PWO jp99 (Japan)	2.80	0.585	4.14	171	>43
PWO Bridgman as-grown (Japan)	2.76	0.63	4.10	174	7
	2.72	0.63	4.15		
PWO Bridgman ann. 600 °C in air (Japan)	2.78	0.64	4.15	179	9
PWO jp96 (Japan)	2.73	0.65	4.12	155	9.3
PWO 106 N ₂ ann.	2.78		4.17	180	0.74
PWO 106 as-grown	2.725		4.15	178	0.66
PWO 154 as-grown	2.77	0.64	4.15	175	1.03
PWO 154 N ₂ -ann.	2.75		4.15	175	0.66
<i>Other crystals</i>					
PWO:50000 ppm Cd (Japan)	2.72	0.69	4.17	197	21.5
	2.775	0.63	4.05		

2. The green emission

The green emission of PbWO_4 was considered in many papers. However, its origin is still under discussion. In [50] oxygen vacancy was recognized as a key defect and the green emission of undoped crystals was ascribed to the WO_3 oxygen-deficient complex anions. The interpretation based on the WO_3 groups was given in many other works (see, e.g., [51–53]). In [54–57], this emission was connected with the inclusions of the raspite structure formed due to the thermal stress appearing in the process of crystal growth. In [5, 34], [58–60] the

green emission was ascribed to the MoO_4^{2-} groups. It was suggested that Mo^{6+} ions are present not only in the Mo^{6+} -doped crystals but also in the undoped crystals as it is difficult to separate chemically very similar Mo^{6+} and W^{6+} ions in the course of the raw material preparation. The presence in the lead-deficient PbWO_4 crystals of the superstructure of the type of $\text{Pb}_{7.5}\text{W}_8\text{O}_{32}$ was reported in [61]. In [62], this superstructure was assumed to be responsible for the green emission. In [63, 64], the green emission was connected with the defects of the type of $\{\text{WO}_4+\text{O}_i\}$.

In some papers (see, e.g., [65], [51–53]), the presence of two green emission bands at RT was reported. In [6, 67], we have also observed two green emissions and found that they are of different origin. Let us denote them as the $G(I)$ and $G(II)$ emissions. The existence of two green emission bands in PbWO_4 crystals, with strongly different characteristics, can explain noticeable deviations reported in different papers as for the shape and position of the excitation/emission bands at RT, temperature dependence of the green emission intensity, spectra and decay kinetics, as well as for the dependences of all these characteristics on the crystal growth and thermal treatment conditions.

We have investigated in detail the characteristics of the $G(I)$ and $G(II)$ emissions in various undoped and doped PbWO_4 crystals containing strongly different concentrations of various impurity and intrinsic defects.

The green emission of the first type (*the $G(I)$ emission*) is observed at low temperatures. Like in the case of the B emission, the positions (2.30–2.37 eV) and FWHM (0.56–0.62 eV) of the $G(I)$ emission band (Fig. 11a, curves 1,1',1''), the positions of its excitation band maximum (Fig. 11a, curve 2) (3.8–4.0 eV) and temperature dependences of the $G(I)$ emission intensity (Fig. 12a, curve 1,2,3) ($T_q=182\text{--}210$ K) are slightly different in different crystals (Table 5).

The decay kinetics of this emission and the parameters of the corresponding excited state are similar to those obtained in [48] for the STE state (Fig. 5), but they are also slightly different in different crystals [6, 67, 68] (Figs. 13a–13c, Table 3, 6). Decay kinetics and the parameter values (see Table 3), in particular spin-orbit splitting energy D , strongly differ for crystals with the scheelite structure (PbWO_4 , PbMoO_4) as compared with those in the crystals with the wolframite (raspite) structure (CdWO_4 , ZnWO_4 , Fig. 13d). It means that the $G(I)$ emission cannot arise from the inclusions of raspite structure. These data indicate that the $G(I)$ emission band can also be a superposition of many closely positioned exciton-like bands.

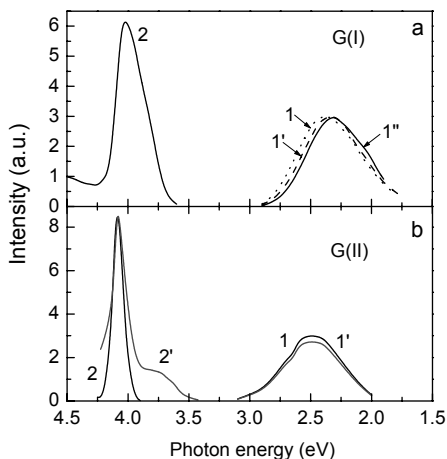


FIG. 11. Emission (curves 1, 1', 1'') and excitation (curves 2, 2') spectra of (a) the G(I) emission of the PWO:1000 ppm Mo (curve 1), PWO:200 ppm Mo (curve 1') and undoped pwo106 (curves 1'', 2) crystals measured at 4.2 K under $E_{exc}=3.7-3.8$ eV; (b) the time-resolved G(II) emission of the undoped annealed at 600 °C in air $PbWO_4$ Bridgman crystal

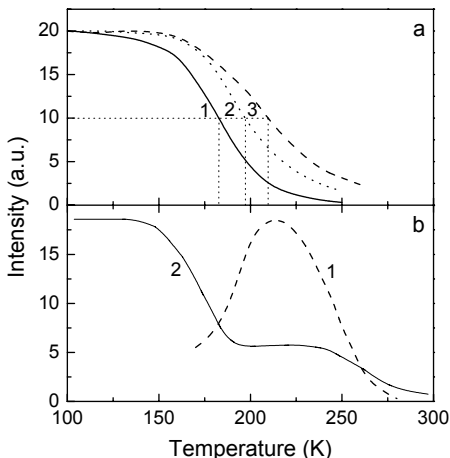


FIG. 12. Temperature dependences of the maximum intensities measured for: (a) the G(I) emission of the PWO:135 ppm Mo (Japan) (curve 1), undoped PWO Bridgman (curve 2) and PWO:200 ppm Mo/100 ppm Nb (curve 3) crystals under $E_{exc}=3.8-3.9$ eV; (b) the G(II) emission under $E_{exc}\sim 4.07$ eV (curve 1) and the blue-green emission under $E_{exc}=4.5$ eV (curve 2) of the undoped pwo106 crystal annealed in the nitrogen atmosphere.

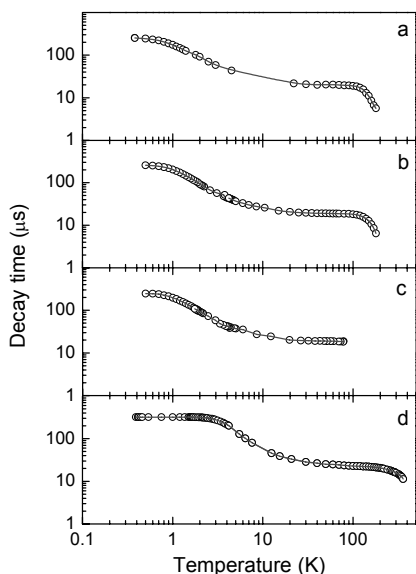


FIG. 13. Temperature dependences of the G(I) emission decay time measured under $E_{exc}=3.8$ eV for three strongly different undoped PWO crystals: (a) pwo154b (50% PbO , 50% WO_3), (b) pwo189h (49% PbO , 51% WO_3), and (c) pwo106 containing large amount of crystal structure defects. For comparison, the $\tau(T)$ dependence of the green intrinsic emission of $CdWO_4$ is also presented (d).

We have assumed [6] that in undoped PbWO_4 crystals this emission arises from the unperturbed and perturbed $(\text{WO}_4)^{2-}$ groups located in the crystal regions of lead-deficient structure $\text{Pb}_{7.5}\text{W}_8\text{O}_{32}$ [61, 69]. Indeed, G(I) emission is intense in lead-deficient crystals grown by the Chochralski method, but in PbWO_4 :5000ppm Cd crystal this emission is suppressed by a strong Cd^{2+} doping [69]. This effect can be explained by the filling of lead vacancies with Cd^{2+} ions and thus removing the lead-deficient scheelite-type structure. In Mo^{6+} -doped crystals, the G(I) emission arises mainly from the $(\text{MoO}_4)^{2-}$ groups [24, 60], however, defects of other origin can contribute into the G(I) emission spectrum of these crystals as well [7].

Table 5. The G emission band maxima (E_m^1) and halfwidths (FWHM), the excitation band maxima ($E_{\text{exc}}^{\text{max}}$), and the B/G(I) emission intensity ratios obtained from the uncorrected spectra measured at 4.2 K (with FEU-79) for various PbWO_4 (PWO) crystals. The temperatures T_q where the emission intensity decreases twice from its value at $T < 80$ K.

Crystal	E_m^1 , eV	FWHM, eV	$E_{\text{exc}}^{\text{max}}$, eV	T_q , K	B/G(I) ratio
<i>Mo-doped crystals</i>					
PWO:135 ppm Mo (Japan)	2.40	0.52	3.89	182	0.22
PWO:1000 ppm Mo	2.40	0.52	~3.90	194	0.19
PWO:200 ppm Mo (87e)	2.37	0.49	3.89	183	0.13
PWO:200 ppm (95b)	2.39	0.52	3.92	190	0.20
PWO:200 ppm Mo/200 ppm Y	2.40	0.52	3.90	184	0.18
PWO:200 ppm Mo/100 ppm Nb	2.38	0.52	3.89	210	~0.08
PWO:800 ppm Mo/ 60 ppm Ce	2.43	0.50	3.9	180	0.40
<i>Undoped crystals</i>					
PWO jp99 (Japan)	~2.35	0.52	~3.90	195	>43
PWO Bridgman as-grown (Japan)	2.35	0.52	~3.90	198	7
PWO Bridgman ann. 600 °C in air (Japan)	~2.38	0.51	~3.90	196	9
PWO 106 N_2 ann.	2.385	0.51	3.98	190	0.74
PWO 106 as-grown	2.35	0.51	3.98	186	0.66
PWO 154 as-grown	2.385	0.53	3.95	185	1.03
PWO 154 N_2 -ann.	2.355	0.53	3.98	180	0.66
<i>Other crystals</i>					
PWO:50000 ppm Cd (Japan)	2.35	0.65	~3.90		21.5

Table 6. Decay times (τ) of the G(I) emission in some PbWO_4 crystals and the intrinsic emission in PbMoO_4 , ZnWO_4 and CdWO_4 crystals [6].

Crystal	$\tau(\mu\text{s})$	τ constant	$\tau(\mu\text{s})$	$\tau(\mu\text{s})$
	at 0.4 K	up to T, K	at 4.2 K	at 77 K
Undoped pwo154b	253	0.6	43	16
Undoped pwo189h	251	0.7	42	17
Undoped pwo106	246	0.6	41	18
PWO:Mo	241	0.6	44	16
PWO:200 ppm Mo	237	0.6	45	16
PWO:5000 ppm Cr	212	0.5	39	16
PWO:50000 ppm Cd	235	0.6	48	18
PbMoO_4	161	0.6	37	16
ZnWO_4	201	1.8	139	38
CdWO_4	320	1.6	200	25

The green emission of the second type (*the G(II) emission*) located at 2.5 eV (Fig. 11b, curves 1) is responsible for the slow (μs -ms) luminescence decay of PbWO_4 . In Fig. 11b, the characteristics of this emission obtained at 220 K from the time-resolved spectra at $t=20\text{--}50\ \mu\text{s}$ after excitation pulse are shown. This emission is excited mainly in a relatively narrow region around 4.1 eV (Fig. 11b, curve 2) but also in the host lattice and in the defect-related (Fig. 11b, curve 2') absorption regions [6, 14, 67], and under these excitations the emission spectra coincide (Fig. 11b, curves 1, 1'). The G(II) emission appears at $T>150\ \text{K}$, its intensity reaches maximum value at 220 K and then decreases (Fig. 12b, curve 1). Under excitation in the exciton region, the activation energy for the G(II) emission increase in the 160–220 K temperature range is equal to the activation energy of the B emission thermal quenching ($\approx 0.20\ \text{eV}$) (compare curves 1 in Figs. 12a and 12b). The G(II) emission is stimulated also in the band-to-band absorption region (see Fig. 12b, curve 2).

This emission is observed only in the crystals, containing isolated lead vacancies V_{Pb} and oxygen vacancies V_{O} . Its intensity decreases as a result of the co-doping of PbWO_4 and $\text{PbWO}_4\text{:Mo}$ crystals with trivalent rare-earth ions (A^{3+}), which leads to the decrease of the number of both the oxygen vacancies (due to the extra positive charge of an A^{3+} ion [70, 71]) and the lead vacancies (due to formation of associates of A^{3+} and V_{Pb} , see also [72]).

Decay curve of the G(II) emission can be approximated by the formula $I(t)\sim t^{-\alpha}$ i.e. in the $\log I$ ($\log t$) coordinates it is a straight line with a slope α (Fig. 14). Detailed study of the dependences of the slope α and the emission intensity on the crystal temperature and irradiation dose (Fig. 15a, 15b) and their comparison with theoretical models of tunnelling processes (see, e.g., [73] and references therein) indicate that under excitation in the exciton region, the G(II) emission accompanies the monomolecular tunneling recombination process,

occurring between isolated (genetic) pairs of electron and hole centers produced without release of electrons into the conduction band. Under excitation in the band-to-band and defect-related regions, the decay kinetics of the G(II) emission is characteristic for the tunneling recombination of chaotically distributed electron and hole centers which are created due to the trapping of optically released free charge carriers at some defects (for more details see [9] and references therein).

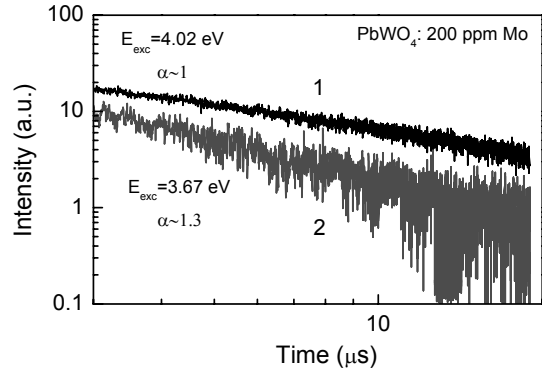


FIG. 14. Decay kinetics of the G(II) emission measured at RT for the PbWO_4 :200 ppm Mo crystal under XeCl (4.02 eV, curve 1) and N_2 (3.67 eV, curve 2) laser excitation.

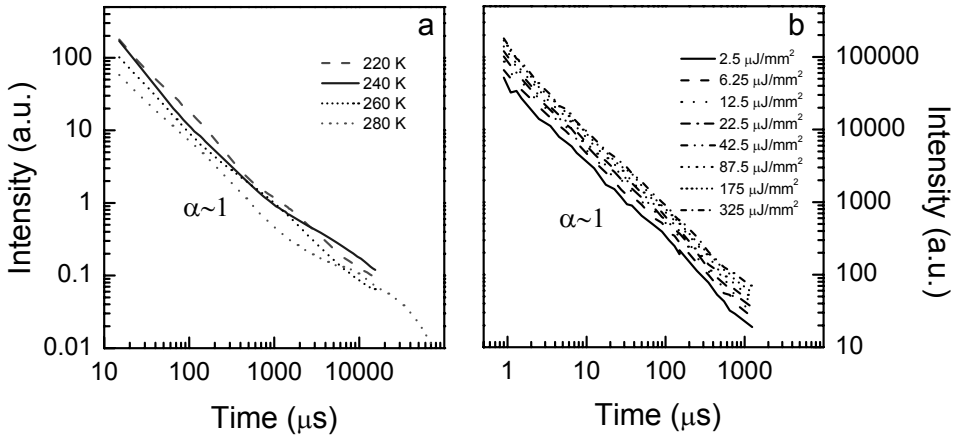


FIG. 15. Decay kinetics of the G(II) emission obtained for the PbWO_4 Bridgman crystal under XeCl-laser excitation at different (a) temperatures and (b) irradiation doses.

3. The red emission

Besides the blue and green emission bands of PbWO_4 crystals, the *red* (R) emission has also been observed (see, e.g., [18, 51, 66]).

In [18], two R emission bands with maxima at 1.8 and 2.0 eV were found at RT and ascribed to F^- centres. In [66], one R band was observed under 4.02 eV and 3.55 eV excitation, peaking at RT near 1.9 eV. This emission was ascribed to complex defects ($\text{Pb}^{3+} + \text{V}_\text{K} + \text{F}^+$) created by W^{6+} ions deficiency in the crystal.

However, the characteristics of R emission were not studied in detail. As in some samples the intensity of the R emission at RT is comparable with the intensity of the blue and green emissions, it may considerably influence the scintillation characteristics of PbWO_4 crystals.

Our studies have shown that the red emission bands of two types are present in the PbWO_4 crystals studied [74]. The *red emission of the first type* – $R(I)$ is observed in most of the undoped and doped crystals studied. Its relative (with respect to the blue band) intensity does not depend on the method of crystal growth, on the presence and concentration of Mo^{6+} and Nb^{5+} ions. It does not change after annealing in air at 600°C of the crystal grown by the Bridgman method. However, strong reduction of the $R(I)$ emission intensity occurs after annealing in the nitrogen atmosphere of the crystal grown by the Czochralski method, and after annealing in air at 1000°C of the crystal grown by the Bridgman method. The red emission is not observed in Cd^{2+} -doped crystals.

The co-doping of the Mo^{6+} -doped crystals with Y^{3+} ions leads to the drastical change of the red emission characteristics. The *red emission of the second type* – $R(II)$ has been observed up to now only in a $\text{PbWO}_4:200 \text{ ppm Mo}^{6+}, 200 \text{ ppm Y}^{3+}$ crystal.

At 4.2 K the *red emission of the first type* is peaking at 1.57 eV, FWHM=0.55 eV (Fig. 16a). The excitation spectrum of the $R(I)$ emission consists of an intense 4.02 eV band and a weaker band near 3.58 eV with a shoulder at 3.3 eV. The dependence of the $R(I)$ emission position on E_{exc} is found, pointing to its complex structure.

Temperature dependence of the $R(I)$ emission intensity is shown in Fig. 17 (curve 1). At RT the $R(I)$ emission band is also complex, it is located at 1.63 eV and excited in the intense 3.85 eV band and in the weaker 3.6–3.3 eV band. In the crystal studied, its maximum intensity at RT is about four times larger than that of the B emission.

In the decay kinetics of the $R(I)$ emission two components are observed at 4.2 K: the main one with decay time $\approx 16 \mu\text{s}$ and the weaker one with decay time $\approx 1.2 \mu\text{s}$. Their emission spectra are located at 1.63 and 1.55 eV, respectively. Near 30 K, the faster component disappears but a new ($19 \mu\text{s}$) component appears, probably, due to the thermally stimulated population of another minimum of the same excited state. Temperature dependences of the decay times of these

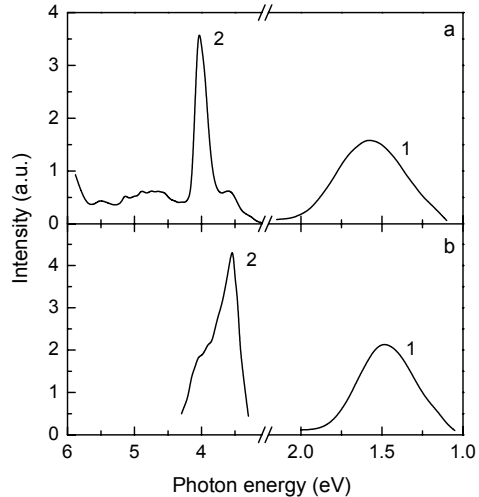


FIG. 16. Emission (curve 1) and excitation (curve 2) spectra at 4.2 K measured for the red emission of the first type (a) and the second type (b).

components are shown in Fig. 18a. The shortening of the decay times with increasing temperature is mainly caused by the thermal quenching of the red emission. At RT the decay times are 18 ns and 66 ns.

At 4.2 K the red emission band of the second type is peaking at 1.48 eV, FWHM=0.41 eV (Fig. 16b). Only the 3.55 eV band is observed in the excitation spectrum of this emission. The higher-energy excitation band cannot be separated due to the presence in the crystal studied of the intense Mo-related absorption at $E_{\text{exc}} > 3.7$ eV. At $E_{\text{exc}} = 3.55$ eV the intensities of the G and R(II) emissions are comparable. As the temperature increases, the maximum of the R(II) emission band is shifting to higher energies (1.55 eV at 180 K) and its intensity decreases, most strongly around 150 K (see Fig. 17, curve 2). At $T > 200$ K the R(II) emission of the second type is practically absent.

In the decay kinetics of this emission, two components are observed with decay times ≈ 290 ns and $30 \mu\text{s}$ at $T < 10$ K (Fig. 18b). The slower component (Fig. 18b, curve 1) is the most intense one, the light sum of the faster component is about 0.3 % from the light sum of the slower one. The emission spectrum of the faster component is shifted by about 0.05 eV to lower energies with respect to the spectrum of the slower component. Decay time of the slower component does not depend much on temperature up to 120 K. Its decrease at higher temperatures is caused by thermal quenching of this emission (see Fig. 17, curve 2). The decay time of the faster component decreases to about 6 ns at 84 K (Fig. 18b, curve 2), and at $T > 100$ K this component is thermally quenched.

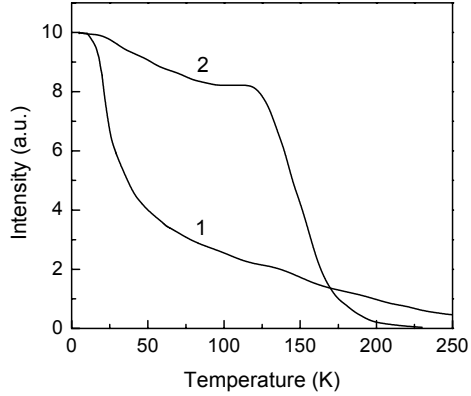


FIG. 17. Temperature dependences of intensity measured for the red emission of the first type (curve 1) and the second type (curve 2).

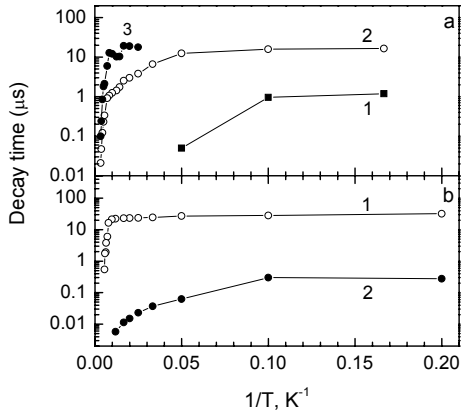


FIG. 18. Temperature dependences of decay times of separate components of the red emission of the first type (a) and of the second type (b).

Basing on literature data [61, 66, 75] and on our results, one may conclude that the R emission of the first type does not arise from impurities. It cannot be connected with WO_3 groups, W^{6+} ions deficiency and Pb-deficient crystal regions. Our experiments showed, that under irradiation of the undoped lead-deficient PbWO_4 crystal at $T > 120$ K in the 4.2–3.7 eV energy range, the intense TSL peak at 225 K and much weaker TSL peaks near 200, 290 and 325 K appear (Fig. 19a). In all the TSL peaks of this crystal, only the R(I) emission is stimulated. The maximum of the defects creation spectrum at 160 K is located at 3.97 eV (Fig. 19, open circles), i.e., it is shifted by about 0.1 eV from the excitation band maximum (4.07 eV) of the B emission measured at the same conditions (Fig. 19, solid line). From the dependence of the $\ln I_{\text{TSL}}$ of the peak at

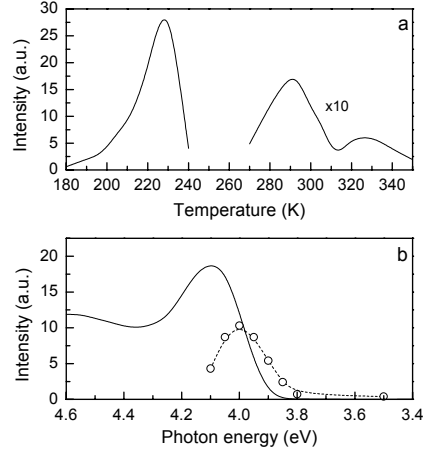


FIG. 19. (a) TSL curve measured for the R emission of undoped crystal after its irradiation at 138 K with $E_{\text{irr}}=4.0$ eV. (b) Excitation spectrum of the B emission (solid line) and the $I_{\text{TSL}}(E_{\text{irr}})$ (points) measured at 160 K with the same slits.

225 K on the reverse irradiation temperature T_{irr} , the activation energy for the defects creation has been calculated ($E_a=0.215$ eV). These data indicate that the defects responsible for the R(I) emission should act as effective traps for holes. As especially intense red emission is observed in undoped lead-deficient PbWO_4 crystal, one may assume that the R emission of *the first type* arises due to the presence of lead vacancies. Strong influence of Y^{3+} on the characteristics of this emission may point to the fact that the R emission of *the second type* can arise from the associates of lead vacancies with Y^{3+} ions.

V. PHOTO-THERMALLY STIMULATED DECAY OF THE EXCITON- AND DEFECT-RELATED STATES

Photo-thermally stimulated decay of the exciton- and defect-related states into stable electron and hole centers was detected earlier by the TSL method in [49] and by the ESR method, in [37, 70, 71, 76, 77]. Recently, these processes were systematically studied by us [7, 8, 10, 74], [12–14], where creation of various electron and hole centers under selective irradiation of PbWO_4 crystals at 80–300 K in the 5.0–3.4 eV energy range reveals itself in the appearance of various TSL peaks. In order to make conclusions about the processes of the exciton- and defect-related states decay, the origin of the TSL peaks was investigated.

1. Characteristics of thermally stimulated luminescence

Thermally stimulated luminescence of X-ray irradiated lead tungstates was intensively studied (see, e.g., [3, 5, 37, 70, 71, 74, 76, 77] and references therein). At the present time, the TSL peaks located at 50 K, around 100 K and at 190–200 K are well identified and ascribed to the thermal destruction of electron $(\text{WO}_4)^{3-}$, $(\text{WO}_4)^{3-}\text{-A}^{3+}$ and $\{\text{Pb}^+\text{-WO}_3\}$ centers, respectively. The peak at 250 K was ascribed to $(\text{MoO}_4)^{3-}$ centers. The peaks at $T > 300$ K were assumed to arise from the associates of $(\text{WO}_3)^-$ with a monovalent impurity ion at the Pb^{2+} site – $(\text{WO}_3)\text{-A}_{\text{Pb}}$ centers or from the associates of $(\text{WO}_3)^-$ with lead vacancies – $(\text{WO}_3)^-\text{-V}_{\text{Pb}}$ centers. Four different types of these centers (W_1 , W_2 , W_3 and W_4) were found. The origin of the 220–230 K peak was unclear. In some papers, the intense peak at 220–230 K was also connected with $(\text{MoO}_4)^{3-}$ centers. The origin and structure of some of the mentioned electron centers was established by the ESR studies carried out for the UV-irradiated samples in [13, 37, 70, 71], [76–79], see Table 7.

The systematic TSL study of more than thirty different crystals carried out in [7, 8, 10, 13] allowed us to conclude that both in the undoped and in the Mo-doped crystals, the G(II) emission is observed in the TSL spectrum at 100–300 K. At higher temperatures, thermally stimulated processes are accompanied with the red emission (see also Chapter IV). The total TSL intensity and the intensity ratio of various peaks at the TSL glow curve are different in different crystals (compare, e.g., Figs. 20a–20c). They are determined mainly by the concentration and type of oxygen (V_O) and lead (V_{Pb}) vacancies in the crystal, which strongly depend on the crystal growth and annealing conditions and on the concentration of A^{3+} ions. In the same crystal, the shape of the TSL glow curve depends strongly on the irradiation energy E_{irr} (Fig. 21a) and irradiation duration t_{irr} (Fig. 21b). The dependences of a TSL peak intensity (I_{TSL}) on E_{irr} (the TSL peak creation spectrum), t_{irr} (the dose dependence) and irradiation temperature (T_{irr}) were studied. It was found that the TSL peaks creation spectra

(Fig. 22) and the dependences of the TSL intensity on the irradiation duration t_{irr} (Fig. 23) are different for different peaks. The values of trap depth E_t , corresponding to each peak, are also different (Table 8). These data indicate that all the TSL peaks located in the 220–250 K range surely arise from different centers.

Table 7. Characteristics of electron centers in PbWO_4 crystals obtained from the ESR data. Details of HF and SHF structure of the ESR spectra are described in [13, 37, 70, 71, 76, 77].

Center	g tensor	Polar and azimuthal angles of axes		HF and SHF Structure	Thermal stability	
		θ	φ			
$(\text{WO}_4)^{3-}$	g_{\parallel} : 1.733	0	0	Interaction with ^{183}W and ^{207}Pb nuclei [37, 77]	40 K $E_a=0.05$ eV	
	g_{\perp} : 1.476	90	0			
$(\text{MoO}_4)^{3-}$	g_{\parallel} : 1.898	0	0	Interaction with $^{95,97}\text{Mo}$ and ^{207}Pb nuclei [77]	250 K $E_a=0.55$ eV	
	g_{\perp} : 1.789	90	0			
$(\text{CrO}_4)^{3-}$	g_{\parallel} : 1.960	0	0	Interaction with ^{207}Pb nuclei [13]	>300 K	
	g_{\perp} : 1.900	90	0			
$(\text{WO}_4)^{3-} - \text{La}^{3+}$	g_1 : 1.770	3	0	Interaction with ^{139}La and ^{207}Pb nuclei [70]	95 K $E_a=0.27$ eV	
	g_2 : 1.542		87			45
	g_3 : 1.471		87			135
			61			13
$\{\text{Pb}^+ - \text{WO}_3\}$ (F^+ center)	g_1 : 1.609	65	118	Interaction with two ^{207}Pb nuclei [71]	185 K $E_a=0.55$ eV	
	g_2 : 1.258	40	241			
	g_3 : 1.220					
$(\text{WO}_3)^- - \text{A}_{\text{pb}}$ (F_A^+ centers)	W_1 : $g_1=1.749$ $g_2=1.703$ $g_3=1.502$	78	337	Interaction with ^{207}Pb nuclei [76]	≈ 360 K	
		76	70			
		161	28			
	W_2 : $g_1=1.809$ $g_2=1.610$ $g_3=1.650$	59	346	--/--	≈ 360 K	
		111	63			
		141	304			
	W_3 : $g_1=1.801$ $g_2=1.708$ $g_3=1.596$	58	13	--/--	≈ 320 K $E_a \approx 0.89$ eV	
		68	117			
		140	55			
	W_4 : $g_1=1.803$ $g_2=1.604$ $g_3=1.717$	59	9	--/--	≈ 320 K $E_a \approx 0.89$ eV	
		128	72			
		127	306			

Let us consider the origin of the 220–230 K peak. This TSL peak consists of at least three components arising from different centers. Its complex structure is evident from the dependences of the peak position on E_{irr} (see e.g., Fig. 24), T_{irr} and t_{irr} . These dependences indicate that the creation spectra, activation energies and dose dependences for the single components of this peak are different. In the undoped as-grown crystals prepared by the Bridgman method, this peak dominates (Fig. 20c, dotted line). After annealing of this crystal in air at 600°C, the intensity of the 220–230 K peak decreases and the intensity of the ≈ 200 K peak increases (solid line). According to [80], in the as-grown crystals the oxygen vacancies of the type of WO_2 and WO prevail, but the annealing transforms these oxygen vacancies into the oxygen vacancies of the type of WO_3 . This allowed us to ascribe the 220–230 K and 200 K peaks to the electron centres connected with the oxygen vacancies of the type of WO_2 , WO and with $\{\text{Pb}^+-\text{WO}_3\}$ centers, respectively [13]. The annealing-induced increase of the number of $\{\text{Pb}^+-\text{WO}_3\}$ centers was confirmed by the ESR method. It was also shown that, unlike the 220–230 K peak, the 250 K peak is observed only in the Mo-containing crystals and only this peak can be ascribed to MoO_4^{3-} centers. Recent ESR studies carried out for the PbWO_4 Bridgman crystal annealed at 600°C in air indicated [14] that also hole centres are thermally destroyed in this temperature range (Fig. 25). Indeed, the decrease in the concentration of $(\text{CrO}_4)^{3-}$ centers, which are surely stable up to $T > 300$ K (Table 7), was observed

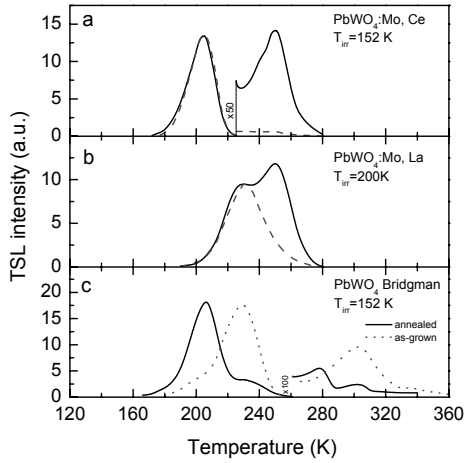


FIG. 20. The TSL glow curves measured with heating rate 0.2 K/s for different PbWO_4 crystals after irradiation in the exciton (4.1 eV) (solid and dotted lines) and defect-related (3.8 eV) (dashed lines) regions.

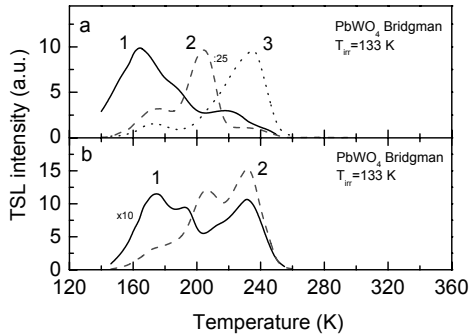


FIG. 21. The TSL glow curves measured with heating rate 0.2 K/s for the annealed PbWO_4 Bridgman crystal after its irradiation at 133 K (a) in the band-to band (4.8 eV, curve 1), exciton (4.12 eV, curve 2 decreased 25 times with respect to the other curves) and defect-related (3.8 eV, curve 3) regions, and (b) at $E_{\text{irr}}=4.05$ eV for $t_{\text{irr}}=5$ min (curve 1, increased 10 times) and $t_{\text{irr}}=20$ min (curve 2).

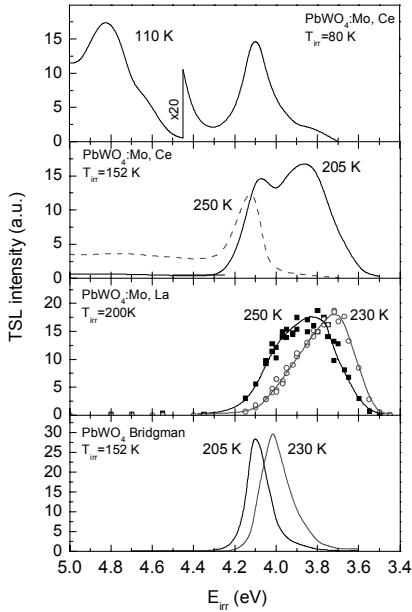


FIG. 22. Some examples of creation spectra of the TSL peaks at 110 K, 205 K, \approx 230 K and 250 K in different PbWO_4 crystals.

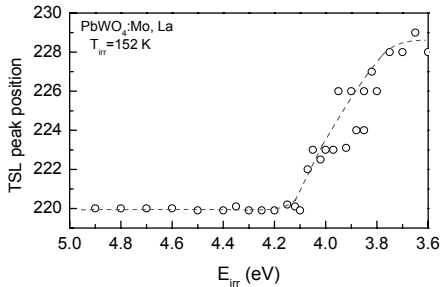


FIG. 24. Dependence of the complex 220–230 K TSL peak position on the irradiation energy E_{irr} measured for the PbWO_4 : 1250 ppm Mo, 80 ppm La crystal after its irradiation at 152 K.

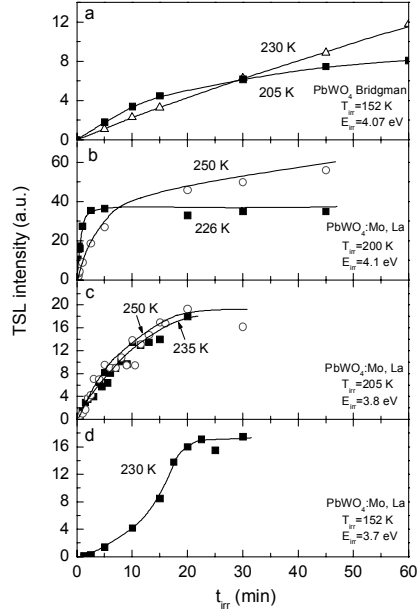


FIG. 23. Dependences of the TSL intensities on the irradiation time t_{irr} measured for the TSL peaks at 205 K, 226 K, 230 K and 250 K after irradiation of the annealed PbWO_4 Bridgman (a) and PbWO_4 :1250 ppm Mo, 80 ppm La (b–d) crystals in the exciton (a, b) and in the defect-related (c, d) energy range.

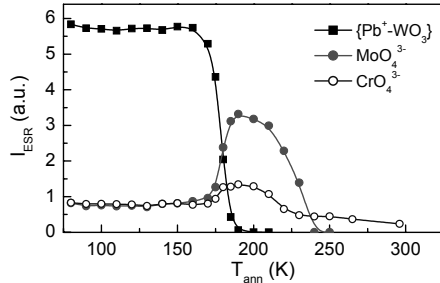


FIG. 25. Temperature dependences of the ESR signal intensities from electron $\{\text{Pb}^+-\text{WO}_3\}$, MoO_4^{3-} and CrO_4^{3-} measured at 16 K for the annealed in air PbWO_4 Bridgman crystal after its irradiation at 80 K in the 3.7–4.0 eV energy range and subsequent heating (for 2 min) at different T_{ann} . A shift in temperature where $\{\text{Pb}^+-\text{WO}_3\}$ and MoO_4^{3-} centers destroy, as compared with the TSL data (see figure 20, solid line and [12]), is caused by different heating conditions used in the ESR and TSL experiments.

at 210–220 K. The decrease in this temperature range of the number of $(\text{MoO}_4)^{3-}$ centers [77] and of the intensity of the recombination G(II) emission (Fig. 12b, curve 1) can also be caused by thermal destruction of hole centers.

Table 8. Characteristics of electron and hole centers in PbWO_4 crystals obtained from the TSL data after crystal irradiation in the exciton (ex^0) and defect-related (def) regions.

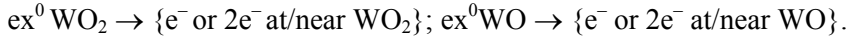
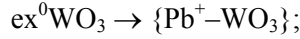
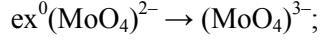
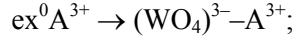
Center	TSL peak, K	E_t (TSL), eV	E_a (ex^0), eV	E_a (def), eV
$(\text{WO}_4)^{3-}-\text{Ce}^{3+}$	≈ 100	0.12	0.01	
$\{\text{Pb}^+-\text{WO}_3\}$	≈ 200	0.46–0.50	0.18–0.20	0.22–0.25
e^- or $2e^-$ at/near WO_2 or WO	$\approx 220\text{--}230$	0.52–0.59	0.19–0.29	0.32–0.38
e^+ at V_{Pb}	≈ 235	0.32	0.20	
$(\text{MoO}_4)^{3-}$	250	0.50–0.52	0.17–0.22	0.15–0.28
$(\text{WO}_3)^--\text{A}_{\text{Pb}}$	305	0.71	0.16	
	335		0.17	

One may assume that in PbWO_4 crystals, electrons are trapped at various V_{O} -related defects and at $(\text{MoO}_4)^{2-}$ groups, but the holes responsible for the G(II) emission, at V_{Pb} -related defects. Co-doping with A^{3+} ions, resulting in the reduction of the number of the isolated vacancies, leads to the suppression of TSL just due to the suppression of the G(II) emission.

2. Creation of electron and hole centers under irradiation in the exciton region

Creation spectra of all the TSL peaks show relatively narrow bands (FWHM ≈ 0.15 eV) (see, e.g., Fig. 22) whose maxima positions are temperature-dependent and different for different TSL peaks (see also [7, 8], [12–14]). Strongly selective creation of each TSL peaks under irradiation in the exciton absorption region indicates that they are created at the decay of different localized exciton states and that the latter process does not result in the release of free electrons. The monomolecular decay kinetics of the G(II) emission observed under this excitation confirms this conclusion. The narrow bands in the creation spectra of different TSL peaks can correspond to various localized excitons. We assume that the excitons of the type of $(\text{WO}_4)^{2-}$ localized near/at A^{3+} ions (ex^0A^{3+}), $(\text{MoO}_4)^{2-}$ groups ($\text{ex}^0(\text{MoO}_4)^{2-}$), and oxygen-deficient complexes of the type of WO_3 (ex^0WO_3), WO_2 (ex^0WO_2) and WO (ex^0WO) can exist in PbWO_4 crystals and that an electron and a hole are released at the photo-thermally stimulated decay of the localized excitons. The released

electron can be immediately trapped at $(\text{WO}_4)^{2-}$ or $(\text{MoO}_4)^{2-}$ groups, at Pb^{2+} ions located close to the oxygen vacancies of the type of WO_3 , around WO_2 and WO complexes, etc. The following processes of electron capture due to exciton decay are assumed to take place [12–14]:



Most probably, two electrons are trapped at the oxygen-deficient complexes of the type of WO_2 and WO as these electron centers do not appear in the ESR spectra.

Under irradiation in the exciton energy range, the dependence of the TSL peak intensity on the irradiation duration is linear at the initial stage and then reaches the saturation (Figs. 23a, 23b).

Activation energies E_a calculated for the TSL peaks creation from the slope of the $\ln I_{\text{TSL}}(1/T_{\text{irr}})$ dependences are shown in Table 8. The E_a value obtained for the ≈ 200 K peak creation due to the decay of the exciton localized near oxygen vacancy (0.22 eV [12]) is close to the value of E_q obtained at $T > 180$ K for thermal quenching of the B emission (≈ 0.20 eV). This fact indicates that thermal quenching of the B emission at $T > 180$ K is caused mainly by the localized exciton decay. At $T < 160$ K, the B emission intensity decreases with much smaller activation energy due to the self-trapped exciton decay with $E_a \approx 0.08$ eV and electron transfer in close $\{(\text{WO}_4)^{2-}\text{-defect}\}$ pairs with $E_a < 0.04$ eV [6]. Thermal quenching of the Mo-related G(I) emission in the PbWO_4 :800 ppm Mo, 60 ppm Ce crystal takes place with the same $E_a \approx 0.22$ eV as that obtained for the decay of the $(\text{MoO}_4)^{2-}$ state in this crystal.

At the localized exciton decay, the mobile holes are most probably released which are further trapped at the V_{pb} -related centers. Recently, the photo-thermally stimulated conductivity was observed under selective excitation in the narrow energy range around 4.1 eV [80]. The creation spectrum and the activation energy $E_a \approx 0.20$ eV obtained for this process are very close to those obtained in [12] for the 205 K TSL peak creation in the exciton absorption region. It means that the photoconductivity could appear due to the decay of the same localized exciton. As free electrons are not released in this process, one can conclude that the hole photoconductivity was observed in [80].

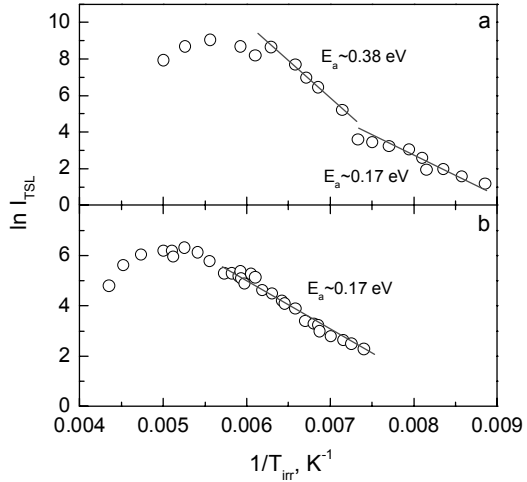
3. Creation of electron and hole centers under irradiation in the defect-related region

Under irradiation at $T_{\text{irr}} > 130$ K in the defect-related absorption region (at 3.7–3.8 eV), various electron centers are created which can be detected by the ESR [77, 79] and the TSL (Fig. 20, see also [7, 12]) methods. Indeed, from the creation spectra of the 205 K, 230 K and 250 K peaks (Fig. 21) it is seen that these TSL peaks are effectively created not only in the exciton but also in the defect-related region. It means that under this excitation, free electrons can be optically released into the conduction band. As a result of their further trapping at some traps, the corresponding electron centers are created. Creation of $\{\text{Pb}^+ - \text{WO}_3\}$ centers, responsible for the 205 K peak, under irradiation of the undoped PbWO_4 Bridgman crystal by the N_2 laser (3.67 eV) at 160 K was detected also by the ESR method. According to [14], this crystal contains Mo ions. Thus, the mentioned centers could be created as a result of electron release from $(\text{MoO}_4)^{2-}$ groups. In [77] it was concluded that electron $(\text{MoO}_4)^{3-}$ centers are effectively produced under irradiation around 3.8 eV due to optical release of holes from $(\text{MoO}_4)^{2-}$ groups.

In $\text{PbWO}_4:\text{Mo}$, optically released electrons can be trapped at $(\text{MoO}_4)^{2-}$ groups, which are known as effective electron traps, and also at some other defects (e.g., $\{\text{Pb}^{2+} - \text{WO}_3\}$, WO_2 , WO , $\text{WO}_3 - \text{A}_{\text{Pb}}$, etc). If the number of the oxygen-vacancy-related traps is negligible, like in A^{3+} -containing crystals [70, 71], the electrons become trapped mainly at $(\text{MoO}_4)^{2-}$. This explains much larger concentration of $(\text{MoO}_4)^{3-}$ centers in $\text{PbWO}_4:\text{Mo}, \text{La}^{3+}$ [77] and especially in $\text{PbWO}_4:\text{Mo}, \text{Ce}^{3+}$ as compared with $\text{PbWO}_4:\text{Mo}$. The optically released hole can be trapped at V_{Pb} -related centers. As it was mentioned above, the tunneling recombination between the electron and V_{Pb} -related hole centers is accompanied with the G(II) emission. In case the hole traps and other electron traps are absent, the fast electron-hole recombination takes place at $(\text{MoO}_4)^{2-}$. Owing to that, in $\text{PbWO}_4:\text{Mo}, \text{A}^{3+}$ crystals the intensity ratio of the fast Mo-related G(I) emission to the slow G(II) emission is much larger than in $\text{PbWO}_4:\text{Mo}$ crystals (see, e.g., reviews [3, 5]). This explains good scintillation characteristics of these systems. At $T > 230$ K, the electrons from $(\text{MoO}_4)^{3-}$ are thermally released into the conduction band. A part of them recombine with hole centers and the TSL peak at 250 K appears. As the hole centers become thermally destroyed at lower temperatures [14], the 250 K peak is always very weak even when the ESR spectra show a large concentration of $(\text{MoO}_4)^{3-}$ centers in the crystals studied. Another part of electrons becomes retrapped at deeper traps (e.g., at $\text{WO}_3 - \text{A}_{\text{Pb}}$ or $\text{WO}_3 - V_{\text{Pb}}$ [76]). The mentioned processes result in the reduction of the number of $(\text{MoO}_4)^{3-}$ centers. However, in the crystals with a small concentration of electron and hole traps, the electrons return back to $(\text{MoO}_4)^{2-}$. Due to the repeated process of electrons thermal release from $(\text{MoO}_4)^{3-}$ and their trapping back at $(\text{MoO}_4)^{2-}$, the equilibrium exists between the $(\text{MoO}_4)^{2-}$

state and the conduction band. In [77] it was found that in the $\text{PbWO}_4:\text{Mo,La}$ crystal the La^{3+} ions at Pb^{2+} sites give rise to free electrons in the conduction band. Owing to that, in this crystal the $(\text{MoO}_4)^{3-}$ centers are observed by the ESR method even after irradiation at RT or after heating the crystal up to RT, and even without prior irradiation of the crystal.

In $\text{PbWO}_4:\text{Mo}$ crystals, containing large amount of various defects responsible for the G(I) emission, not only $(\text{MoO}_4)^{2-}$ groups but also some other defect centers can be ionized by photons of the 3.7–3.8 eV energy. Indeed, it was found in [7, 8] that in different $\text{PbWO}_4:\text{Mo}$ crystals, strongly different E_a values are obtained for the creation of the same TSL peaks in the same energy range (in spite of the fact that $(\text{MoO}_4)^{3-}$ centers of only one type exist [77]). Even in the same crystal, the E_a values for different TSL peaks creation with the same irradiation energy are strongly different. For example, at $E_{\text{irr}}=3.75$ eV, the activation energy for the 220–230 K peak creation is $E_a=0.38$ eV (Fig. 26a), and for the 250 K peak creation



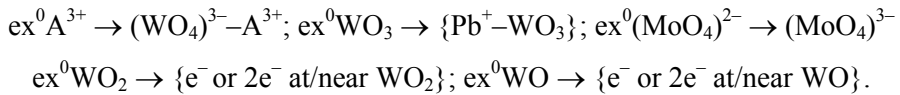
$E_a=0.17$ eV (Fig. 26b) (see also Table 8). The low-temperature stage with $E_a=0.17$ eV observed in Fig. 26a can indicate that the electron centers responsible for the 220–230 K peak are created at the decay of both $(\text{MoO}_4)^{2-}$ centers (with $E_a=0.17$ eV) and some other defects (with $E_a=0.38$ eV). The dose dependences can also be different for different TSL peaks creation with the same irradiation energy. For example, the superlinear dependence of the TSL intensity on irradiation duration is obtained for the electron 220–230 K peak in the $\text{PWO}:\text{Mo,La}$ crystal (Fig. 23d). That may mean that the electron centers responsible for this peak are created due to the two-photon process, i.e., the ionization of a $(\text{MoO}_4)^{3-}$ center, created by the first photon (as a result of a hole release), takes place by the second photon. The same, linear and then sublinear, dependence observed for the 250 K and ≈ 235 K peaks creation (Fig. 23c) may mean that both the corresponding electron and hole centers are created by one photon.

SUMMARY

In the present work, a systematic study of the luminescence and photo-thermally stimulated defects creation processes, occurring in lead tungstate crystals under their selective UV irradiation, was carried out in a wide temperature range by the methods of steady-state and time-resolved luminescence spectroscopy and also by the TSL and ESR methods. The data obtained at the investigation of more than thirty undoped and doped PbWO_4 crystals, containing different concentrations of various impurity and crystal structure defects, grown by different methods, in different laboratories, and annealed at different conditions were compared.

As a result, the complex structure and the nature of the blue, green and red spectral bands observed in the luminescence spectrum of PbWO_4 crystals were established and the parameters of the corresponding excited states determined. It was found that the B and G(I) emission bands are of the exciton-like origin and arise from the $(\text{WO}_4)^{2-}$ groups, unperturbed or perturbed by various defects and located in the regular and in the lead-deficient crystal regions of sheelite structure, respectively. The slow G(II) emission accompanies photo- and thermally stimulated tunneling recombination processes in different (genetic or stochastic) optically created pairs of V_{0-} and $(\text{MoO}_4)^{3-}$ -related electron centers and V_{Pb} -related hole centers. Thermal quenching of the B and the G(I) emission is mainly caused by the decay of the corresponding exciton states. Thermal quenching of the G(II) emission is caused by thermal destruction of the corresponding hole centers. The R(I) emission is most probably related to lead vacancy containing centers, acting as hole traps, while R(II) emission can arise from the associates of lead vacancies with Y^{3+} ions.

Various localized exciton states (e.g., the excitons of the type of $(\text{WO}_4)^{2-}$ localized near A^{3+} ions, oxygen vacancies of the type of WO_3 , WO_2 or WO , and $(\text{MoO}_4)^{2-}$ groups) were identified and their photo-thermally stimulated decay into electron and hole centers was found. The decay of the localized excitons was assumed to result in the following processes:



It was found that the creation of electron centers in these processes takes place without release of the free electrons. The optically released mobile holes can be responsible for the photoconductivity observed under irradiation in the localized exciton absorption region at $T > 150$ K.

It was concluded that at the photo-thermally stimulated decay of the self-trapped excitons and defect-related states, free charge carriers are released.

Lead and oxygen vacancies were found to play an important role in the trapping of holes and electrons, respectively, and in the optically and thermally

stimulated recombination processes. Co-doping with stable A^{3+} ions reduces the number of the isolated vacancies. This leads to both a strong suppression of the slow (μs - ms) tunnelling recombination G(II) luminescence and the enhancement of the fast (2–4 ns at RT) B and G(I) emissions. As a result, considerable improvement of scintillation characteristics of PbWO_4 crystals takes place.

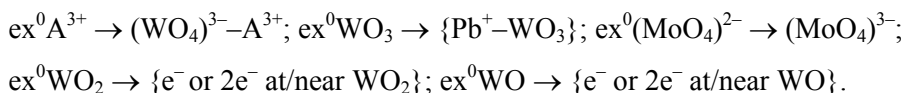
The conclusion was also made that the study of dependences of the number of various electron and hole centers, created under selective UV irradiation, on irradiation energy, irradiation temperature and irradiation duration, carried out at the same samples and in the comparable conditions by both the ESR and TSL methods, is an excellent method for investigation of the origin of these centers and the mechanisms of their creation.

SUMMARY IN ESTONIAN

Käesolevas töös on uuritud luminesentsi ja foto-termostimuleeritud defekti-tekke protsesse, mis leiavad aset pliivolframaatkristallide (PbWO_4) selektiivsel kiiritamisel ultravioletses spektripiirkonnas. Uuringud on läbi viidud laias temperatuurivahemikus statsionaarse- ja aeglahutusega luminesentspektroskoopia meetodil ning termostimuleeritud luminesentsi (TSL) ja elektronide paramagnetilise resonantsi (EPR) meetoditel. On võrreldud andmeid, mis olid saadud rohkem kui kolmekümne aktiveerimata ja aktiveeritud PbWO_4 kristalli uurimisel, mis olid valmistatud erinevates laborites erinevate meetoditega ja erinevates tingimustes tehniliselt töödeldud ning sisaldasid erinevaid lisandiioonide ja kristalli struktuuridefektide kontsentratsioone.

Töö tulemusena tehti kindlaks PbWO_4 kristallide sinise, roheline ja punase kiirguse loomus ja selgitati välja vastavate luminesentsitsentrite ergastatud seisundite struktuur, parameetrid ja dünaamika. Leiti, et sinise B- ja roheline G(I)-kiirguse ribad omavad eksitoni loomust ja on pärit häirimata või erinevate defektide poolt häiritud $(\text{WO}_4)^{2-}$ -gruppidest, mis paiknevad vastavalt regulaarsetes ja pliidefitsiidiga šeliidi struktuuriga kristallialades. Näidati, et aeglane roheline G(II)-kiirgus tekib foto-termostimuleeritud tunnelrekombinatsioon-protsessides erinevates (geneetilistes või stohhastilistes) optiliselt loodud paardes, mis koosnevad hapniku vakantsiga (V_0) seotud või $(\text{MoO}_4)^{3-}$ elektron-tsentritest ning pliivakantsiga (V_{Pb}) seotud auktsentritest. Tehti järeldus, et B- ja G(I)-kiirguste termilise kustumise peamiseks põhjuseks on vastavate eksiton-seisundite lagunemine, aga G(II)-kiirguse termiline kustumine võib olla seotud vastavate auktsentrite termilise lagunemisega. Punane R(I)-kiirgus on kõige tõenäolisemalt seotud pliivakantse (V_{Pb}) sisaldavate tsentritega, mis võivad haarata auke, aga R(II)-kiirgus võib olla seotud assotsiaatidega $\{V_{\text{Pb}}-Y^{3+}\}$.

Identifitseeriti erinevad lokaliseerunud eksitonide seisundid (näiteks, $(\text{WO}_4)^{2-}$ -tüüpi eksitonid, mis on lokaliseerunud A^{3+} ioonide, WO_3^- , WO_2^- või WO -tüüpi hapniku vakantside ning $(\text{MoO}_4)^{2-}$ -gruppide kõrval) ja leiti nende foto-termostimuleeritud lagunemine elektron- ja auktsentriteks. Oletati, et lokaliseerunud eksitonide lagunemisel toimuvad järgmised protsessid:



Leiti, et vabu elektrone nendes protsessides ei teki. Optiliselt loodud mobiilsed augud võivad aga vastutada fotojuhtivuse eest, mis tekib kristalli kiiritamisel lokaliseerunud eksitoni neeldumispkiirkonnas temperatuuril $T > 150$ K.

Tehti järeldus, et autolokaliseerunud eksitonide ning defektiseisundite foto-termostimuleeritud lagunemisel tekivad vabad laengukandjad.

Leiti, et plii ja hapniku vakantsid mängivad olulist rolli aukude ja elektronide haaramisel, seega ka foto- ja termostimuleeritud rekombinatsioon-

protsessides. Kristalli legeerimine stabiilsete A^{3+} -ioonidega vähendab isoleeritud vakantside arvu. See vähendab tugevasti ka aeglase (μs - ms) tunnelrekombinatsioon- G(II)-luminesentsi intensiivsust ja suurendab kiire (2–4 ns) B- ja G(I)-kiirguse intensiivsust, mille tulemuseks on märgatav PbWO_4 -kristallide stsintsillatsiooni-karakteristikute paranemine.

Tehti järeldus, et erinevate selektiivsel UV-kiiritamisel tekitatud elektron- ja auktsentrite arvu sõltuvuse uurimine kiiritamise energiast, temperatuurist ja kestvusest, mis on läbi viidud samade objektide jaoks võrreldavates tingimustes nii TSL kui ka EPR meetodil, on suurepäraseks meetodiks nende tsentrite loomuse ja nende moodustumise mehhanismide väljaselgitamisel.

REFERENCES

- [1] V. G. Baryshevski, M. Korzhik, V. I. Moroz, V. B. Pavlenko, A. F. Lobko, A. A. Fedorov, et al., “Single crystals of tungsten compounds as promising material for the total absorption detectors of the e.m. calorimeters”, *Nucl. Instrum. Methods. Phys. Res. A*, **322**, 231, 1992.
- [2] M. Kobayashi, M. Ishii, Y. Usuki, and H. Yahagi, “Scintillation characteristics of PbWO₄ single crystals at room temperature”, *Nucl. Instrum. Methods. Phys. Res. A*, **333**, 429, 1993.
- [3] M. Nikl, “Wide band gap scintillation materials: progress in the technology and material understanding”, *Phys. Stat. Sol. A*, **178**, 595, 2000.
- [4] M. Nikl, “Energy transfer phenomena in the luminescence of wide band-gap scintillators”, *Phys. Stat. Sol. A*, **202**, 201, 2005.
- [5] A. A. Annenkov, M. V. Korzhik, and P. Lecoq, “Lead tungstate scintillation material”, *Nucl. Instrum. Methods Phys. Res. A*, **490**, 30, 2002.
- [6] V. Babin, P. Bohacek, A. Krasnikov, M. Nikl, A. Stolovits, and S. Zazubovich, “Origin of green luminescence in PbWO₄ crystals”, *J. Lumin.*, **124**, 113, 2007.
- [7] P. Bohacek, P. Fabeni, A. Krasnikov, M. Nikl, G. P. Pazzi, C. Susini, and S. Zazubovich, “Defects in UV-irradiated PbWO₄:Mo crystals monitored by TSL measurements”, *Phys. Stat. Sol. C*, **2**, 547, 2005.
- [8] P. Bohacek, P. Fabeni, A. Krasnikov, M. Nikl, G. P. Pazzi, C. Susini, and S. Zazubovich, “Defects creation under UV irradiation of PbWO₄ crystals”, *Rad. Protect. Dosimetry*, **119**, 164, 2006.
- [9] P. Fabeni, V. Kiisk, A. Krasnikov, M. Nikl, G. P. Pazzi, I. Sildos, and S. Zazubovich, “Tunneling recombination processes in PbWO₄”, *Phys. Stat. Sol. C*, **4**, 918, 2007.
- [10] P. Fabeni, A. Krasnikov, V. V. Laguta, M. Nikl, G. P. Pazzi, C. Susini, and S. Zazubovich, “Origin of TSL peaks located at 200–250 K in UV-irradiated PbWO₄ crystals”, *Rad. Measur.*, **42**, 807, 2007.
- [11] A. Krasnikov, M. Nikl, and S. Zazubovich, “Processes resulting in thermal quenching of the blue emission in PbWO₄ crystals”, in *Proc. of the Int. Conf. on Inorganic Scintillators and their Use in Scientific and Industrial Applications*, SCINT2005, Ukraine, Kharkov, 362, 2006.
- [12] A. Krasnikov, M. Nikl, S. Zazubovich, “Localized excitons and defects in PbWO₄ single crystals: a luminescence and photo-thermally stimulated disintegration study”, *Phys. Stat. Sol. B*, **243**, 1727, 2006.
- [13] A. Krasnikov, V. V. Laguta, M. Nikl, and S. Zazubovich, “Localized excitons and their decay into electron and hole centers in the PbWO₄ single crystals grown by the Bridgman method”, *J. Phys.: Condens. Matter*, 2007, to be published.
- [14] V. V. Laguta, M. Nikl, and S. Zazubovich, “Luminescence and decay of excitons in lead tungstate crystals”, *Rad. Measur.*, **42**, 515, 2007.
- [15] Blasse G. and Grabmaier B. C. “Luminescent Materials”, *Springer-Verlag*, 226p, 1994.
- [16] Deych R., Dobbs J., Marcovici S. and Tuval B. “Cadmium tungstate detector for computed tomography”, in *Proc. of the Int. Conf. on Inorganic Scintillators and Their Applications*, SCINT95, Netherlands, Delft, 36, 1996.

- [17] Lecoq P., “The lead tungstate calorimeter of the CMS experiment at LHC”, in *Proc. of the Int. Conf. on Inorganic Scintillators and Their Applications*, SCINT95, Netherlands, Delft, 52, 1996.
- [18] Grasser R., Schramann A. and Vlachos K., “A renewed investigation of the luminescence of PbMoO_4 and PbWO_4 ”, presented at the *Int. Conf. on Lumin.*, ICL 93, Storrs, USA, M5–9, 1993.
- [19] A. Fyodorov, M. Korzhik, O. Missevitch, V. Pavlenko, V. Kachanov, A. Singovsky, A. N. Annenkov, V. A. Ligun, J. P. Peigneux, J. P. Vialle, J. L. Faure and F. Binon, “Progress in PbWO_4 scintillating crystals”, *Rad. Measur.*, **26**, 107, 1996.
- [20] Лимаренко Л. Н., Носенко А. Е., Пашковский М. В., Футорский Д. Л., “Влияние структурных дефектов на физические свойства вольфрамов”, *Львов, «Вища школа»*. 160с., 1978.
- [21] Демьянец Л. Н., Илюхин В. В., Чичагов А. В. и Белов Н. В., “О кристаллохимии изоморфных замещений в молибдатах и вольфраматах двухвалентных металлов”, *Неорганические материалы*, **3**, 2221, 1967.
- [22] R. Grasser, E. Pitt, A. Scharmann, G. Zimmerer, “Optical properties of CaWO_4 and CaMoO_4 crystals in the 4 to 25 eV region”, *Phys. Stat. Sol. B*, **69**, 359, 1975.
- [23] Y. Zang, N. A. W. Holzwarth, R. T. Williams, Electronic band structures of the scheelite materials CaMoO_4 , CaWO_4 , PbMoO_4 , and PbWO_4 , *Phys. Rev. B*, **57**, 12738, 1998.
- [24] R. Williams, Y. Zhang, Y. Abraham, N. Holzwarth, “Electronic structure of pure and defective PbWO_4 , CaWO_4 and CdWO_4 ”, in *Proc. of the Int. Conf. on Inorganic Scintillators and Their Applications*, SCINT99, Russia, Moscow, 118, 2000.
- [25] Y. Abraham, N. Holzwarth, and R. Williams, “Electronic Structure and Optical Properties of CdMoO_4 and CdWO_4 ”, *Phys. Rev. B*, **62**, 1733, 2000.
- [26] M. Ishii and M. Kobayashi, “Single crystals for radiation detectors”, *Prog. Cryst. Growth & Charact.*, **23**, 245, 1992.
- [27] M. Nikl, “Scintillation detectors for X-rays”, *Meas. Sci. Technol.*, **17**, R37–R54, 2006.
- [28] M. Kobayashi, M. Ishii and Y. Usuki, “Comparison of radiation damage in different PbWO_4 scintillating crystals”, *Nucl. Instrum. Methods. Phys. Res. A*, **406**, 442, 1998.
- [29] K. Hara, M. Ishii, M. Kobayashi, M. Nikl, H. Takano, M. Tanaka, K. Tanji and Y. Usuki, “La-doped PbWO_4 scintillating crystals grown in large ingots”, *Nucl. Instrum. Methods. Phys. Res. A*, **414**, 325, 1998.
- [30] M. Nikl, P. Bohacek, A. Vedda, M. Martini, G. P. Pazzi, P. Fabeni, and M. Kobayashi, “Efficient Medium-Speed $\text{PbWO}_4:\text{Mo},\text{Y}$ Scintillator”, *Phys. Stat. Sol. A*, **182**, R3–R5, 2000.
- [31] A. A. Annenkov, A. E. Borisevich, A. Hofstaetter, M. V. Korzhik, P. Lecoq, V. D. Ligun, O. V. Missevitch, R. Novotny, and J. P. Peigneux, “Improved light yield of lead tungstate scintillators”, *Nucl. Instrum. Methods. Phys. Res. A*, **450**, 71, 2000.
- [32] M. Nikl, P. Bohacek, E. Mihokova, N. Solovieva, A. Vedda, M. Martini, G. P. Pazzi, P. Fabeni, and M. Kobayashi, “Complete characterization of doubly doped $\text{PbWO}_4:\text{Mo},\text{Y}$ scintillators”, *J. Appl. Phys.*, **91**, 2791, 2002.
- [33] J. Pejchal, P. Bohacek, M. Nikl, V. Mucka, M. Pospisil, M. Kobayashi, and Y. Usuki, “Radiation damage of doubly doped $\text{PbWO}_4:(\text{Mo}, \text{A}^{3+})$ scintillator”, *Rad. Measur.*, **38**, 385, 2004.

- [34] A. Hofstaetter, R. Oeder, A. Scharmann, D. Schwabe, B. Vitt, "Paramagnetic Resonance and Thermoluminescence of the $\text{PbWO}_4/\text{PbMoO}_4$ Mixed Crystal System", *Phys. Stat. Sol. B*, **89**, 375, 1978.
- [35] S. Zazubovich, "Polarization spectroscopy of ns^2 impurity ions in alkali halides", *Int. Journal of Modern Physics B*, **8**, 985, 1994.
- [36] M. Nikl, E. Mihokova, K. Nitsch, "Photoluminescence & decay kinetics of Cs_4PbCl_6 single crystals", *Solid State Commun.*, **84**, 1089, 1992.
- [37] V. V. Laguta, J. Rosa, M. I. Zaritskii, M. Nikl, and Y. Usuki, "Polaronic WO_4^{3-} centers in PbWO_4 single crystals", *J. Phys.: Condens. Matter*, **10**, 7293, 1998.
- [38] P. Fabeni, R. Linari, G. P. Pazzi, A. Ranfagni, L. Salvini, "Temperature dependence of the time-resolved emissions of CsI:TI ", *Rad. Eff. Def. Solids*, **119–121**, 307, 1991.
- [39] L. Grigorjeva, D. Millers, S. Chernov, M. Nikl, Y. Usuki and V. Pankratov, "The study of time-resolved absorption and luminescence in PbWO_4 crystals", *Nucl. Instrum. Methods Phys. Res. B*, **166–167**, 329, 2000.
- [40] V. Pankratov, L. Grigorjeva, D. Millers, S. Chernov and A. S. Voloshinovskii, "Luminescence center excited state absorption in tungstates", *J. Lumin.*, **94–95**, 427, 2001.
- [41] D. Millers, S. Chernov, L. Grigorjeva and V. Pankratov, "The energy transfer to the luminescence centers in PbWO_4 ", *Rad. Measur.*, **29**, 263, 1998.
- [42] D. Millers, S. Chernov, L. Grigorjeva, A. Popov, E. Auffray, I. Dafinei, P. Lecoq and M. Schneegans, "Time-resolved luminescence and induced absorption in PbWO_4 ", *J. Lumin.*, **72–74**, 693, 1997.
- [43] W. Van Loo, D. J. Wolterink, "Luminescence decay of lead tungstate and lead molybdate", *Phys. Letters A*, **47**, 83–84, 1974.
- [44] M. Nikl, K. Nitsch, K. Polak, E. Mihokova, I. Dafinei, E. Auffray, P. Lecoq, P. Reiche, R. Uecker, G. P. Pazzi, "Slow components in the photoluminescence and scintillation decays of PbWO_4 single crystals", *Phys. Stat. Sol. B*, **195**, 311, 1996.
- [45] G. P. Pazzi, P. Fabeni, M. Nikl, P. Bohacek, E. Mihokova, A. Vedda, M. Martini, M. Kobayashi, Y. Usuki, "Delayed recombination luminescence in lead tungstate (PWO) scintillating crystals", *J. Lumin.*, **102–103**, 791–796, 2003.
- [46] M. Nikl, P. Bohacek, E. Mihokova, V. Babin, A. Stolovich, A. Krasnikov, S. Zazubovich, G. P. Pazzi, P. Fabeni, A. Vedda, M. Martini, "Excited state dynamics of luminescence centers in PbWO_4 single crystals", *Functional Materials*, **10**, 1, 2003.
- [47] W. van Loo, "Luminescence of lead molybdate and lead tungstate", *Phys. Stat. Sol. A*, **27**, 565; **28**, 227, 1975.
- [48] M. Nikl, P. Bohacek, E. Mihokova, M. Kobayashi, M. Ishii, Y. Usuki, V. Babin, A. Stolovits, S. Zazubovich, M. Bacci, "Excitonic emission of scheelite tungstates AWO_4 ($A=\text{Pb, Ca, Ba, Sr}$)", *J. Lumin.*, **87–89**, 1136, 2000.
- [49] V. Mürk, M. Nikl, E. Mihokova, and K. Nitsch, "A study of electron excitations in CaWO_4 and PbWO_4 single crystals", *J. Phys.: Condens. Matter*, **9**, 249, 1997.
- [50] J. A. Groenink, G. Blasse, "Some new observations on the luminescence of PbMoO_4 and PbWO_4 ", *J. Solid State Chem.*, **32**, 9, 1980.
- [51] M. V. Korzhik, V. B. Pavlenko, T. N. Timoschenko, V. A. Katchanov, A. V. Singovskii, A. N. Annenkov, V. A. Ligun, I. M. Solskii, J.-P. Peigneux,

- “Spectroscopy and origin of radiation centers and scintillation in PbWO₄ single crystals”, *Phys. Stat. Sol. A*, **154**, 779, 1996.
- [52] A. Annenkov, E. Auffray, M. Korzhik, P. Lecoq, J.-P. Peigneux, “On the origin of the transmission damage in lead tungstate crystals under irradiation”, *Phys. Stat. Sol. A*, **170**, 47, 1998.
- [53] A. N. Annenkov et al. *Zh. Prikl. Spectrosk.*, **61**, 83 (1994) (in Russian).
- [54] M. Itoh, M. Fujita, “Optical properties of scheelite and raspite PbWO₄ crystals”, *Phys. Rev. B*, **62**, 12825, 2000.
- [55] M. Itoh, D. L. Alov, M. Fujita, “Exciton Luminescence of Scheelite- and Raspite-structured PbWO₄ Crystals”, *J. Lumin.*, **87–89** 1243, 2000.
- [56] D. L. Alov, N. V. Klassen, N. N. Kolesnikov, S. Z. Shmurak, “Structure dependence of the emission in PbWO₄”, in *Proc. of Int. Conf. on Inorganic Scintillators and Their Applications*, SCINT95, Netherlands, Delft, 267, 1996.
- [57] D. L. Alov and S. I. Rybchenko, “Luminescence properties of raspite PbWO₄”, *Mater. Sci. Forum*, **239–241**, 279, 1997.
- [58] M. Kobayashi, M. Ishii, K. Harada, Y. Usuki, H. Okuno, H. Shimizu, T. Yazawa, “Scintillation and phosphorescence of PbWO₄ crystals”, *Nucl. Instr. Meth. Phys. Res. A*, **373**, 333, 1996.
- [59] R. Y. Zhu, D. A. Ma, H. B. Newman, C. L. Woody, J. A. Kierstead, S. P. Stoll, P. W. Levy, “A study on the properties of lead tungstate crystals”, *Nucl. Instr. Meth. Phys. Res. A*, **376**, 319, 1996.
- [60] M. Böhm, A. E. Borisevich, G. Yu. Drobychev, A. Hofstaetter, O. V. Kondratiev, M. V. Korzhik, M. Luh, B. K. Meyer, J.-P. Peigneux, A. Scharmann, “Influence of Mo impurity on the spectroscopic and scintillation properties of PbWO₄ crystals”, *Phys. Stat. Sol. A*, **167**, 243, 1998.
- [61] J. M. Moreau, R. E. Gladyshevskii, Ph. Galez, J. P. Peigneux, and M. V. Korzik, “A new structural model for Pb-deficient PbWO₄”, *J. Alloys & Comp.*, **284**, 104, 1999.
- [62] M. V. Korzhik, “PbWO₄ scintillator. Current status of R&D”, in *Proc. Int. Conf. on Inorganic Scintillators and their Application*, SCINT95, Netherlands, Delft, 241, 1996.
- [63] C. Shi, Y. Wei, X. Yang, D. Zhou, C. Guo, J. Liao, H. Tang, “Spectral properties and thermoluminescence of PbWO₄ crystals annealed in different atmospheres”, *Chem. Phys. Letters*, **328**, 1, 2000.
- [64] Y. Huang, X. Q. Feng, W. Zhu and Z. Man, “Energy transfer and annealing behavior of luminescence in Dy³⁺-doped PbWO₄ single crystal”, *J. Crystal Growth*, **250**, 431, 2003.
- [65] P. Lecoq, I. Dafinei, E. Auffray, M. Schneegans, M. V. Korzhik, O. V. Mishevitch, V. B. Pavlenko, A. A. Fedorov, A. N. Annenkov, V. L. Kostylev, V. D. Ligun, *Nucl. Instr. Meth. Phys. Res. A*, **365**, 291, 1995.
- [66] P. Lecoq, I. Dafinei, E. Auffray, M. Schneegans, M. V. Korzhik, O. V. Mishevitch, V. B. Pavlenko, A. A. Fedorov, A. N. Annenkov, V. L. Kostylev, V. D. Ligun, “Lead tungstate (PbWO₄) scintillators for LHC EM calorimetry”, *Nucl. Instr. Meth. Phys. Res. A*, **365**, 291, 1995.
- [67] V. Babin, P. Bohacek, E. Bender, A. Krasnikov, E. Mihokova, M. Nikl, N. Senguttuvan, A. Stolovits, Y. Usuki, and S. Zazubovich, “Decay kinetics of the green emission in tungstates and molybdates”, *Rad. Measur.*, **38**, 533, 2004.

- [68] E. Mihokova, M. Nikl, P. Bohacek, V. Babin, A. Krasnikov, A. Stolovits, S. Zazubovich, A. Vedda, M. Martini, T. Grabowski, “Decay kinetics of the green emission in $\text{PbWO}_4\text{:Mo}$ ”, *J. Lumin.*, **102**, 618, 2003.
- [69] A. Krasnikov, M. Nikl, A. Stolovits, Y. Usuki, S. Zazubovich, “Luminescence of the $\text{PbWO}_4\text{:5% Cd}$ crystal”, *Phys. Stat. Sol. C*, **2**, 77, 2005.
- [70] V. V. Laguta, M. Martini, F. Meinardi, A. Vedda, A. Hofstaetter, B. K. Meyer, M. Nikl, E. Mihokova, J. Rosa, and Y. Usuki, “Photoinduced $(\text{WO}_4)^{3-}\text{-La}^{3+}$ center in PbWO_4 : electron spin resonance and thermally stimulated luminescence study”, *Phys. Rev. B*, **62**, 10109, 2000.
- [71] V. V. Laguta, M. Martini, A. Vedda, M. Nikl, E. Mihokova, P. Bohacek, J. Rosa, A. Hofstaetter, B. K. Meyer, and Y. Usuki, “Photoinduced Pb^+ center in PbWO_4 : Electron spin resonance and thermally stimulated luminescence study”, *Phys. Rev. B*, **64**, 165102, 2001.
- [72] B. Han, X. Q. Feng, G. Hu, P. Wang, and Z. Yin, “Observation of dipole complexes in $\text{PbWO}_4\text{:La}^{3+}$ single crystals”, *J. Appl. Phys.*, **84**, 2831, 1998.
- [73] V. Grabovskis and I. Vitols, “Tunneling recombination luminescence in KBr and KCl”, *J. Lumin.*, **20**, 337, 1979.
- [74] P. Bohacek, N. Senguttuvan, V. Kiisk, A. Krasnikov, M. Nikl, I. Sildos, Y. Usuki, and S. Zazubovich, “Red emission of PbWO_4 crystals”, *Rad. Measur.*, **38**, 623, 2004.
- [75] N. Senguttuvan, M. Ishii, K. Tanji, T. Kittaka, Y. Usuki, M. Kobayashi, and M. Nikl, “Influence of annealing on the optical properties of PbWO_4 single crystals grown by the Bridgman method”, *Jpn. J. Appl. Phys.*, **39**, 5134, 2000.
- [76] V. V. Laguta, M. Martini, A. Vedda, E. Rosetta, M. Nikl, E. Mihokova, J. Rosa, and Y. Usuki, “Electron traps related to oxygen vacancies in PbWO_4 ”, *Phys. Rev. B*, **67**, 205102, 2003.
- [77] V. V. Laguta, A. Vedda, D. Di Martino, M. Martini, M. Nikl, E. Mihokova, J. Rosa, and Y. Usuki, “Electron capture in $\text{PbWO}_4\text{:Mo}$ and $\text{PbWO}_4\text{:Mo,La}$ single crystals: ESR and TSL study”, *Phys. Rev. B*, **71**, 235108, 2005.
- [78] M. Böhm, A. Hofstaetter, M. Luh, B. K. Meyer, A. Scharman, M. V. Korzhik, O. V. Kondratiev, A. E. Borisevich, V. V. Laguta, P. Lecoq, and E. Auffray-Hillemans, “Thermally stimulated luminescence properties of lead tungstate crystals”, in *Proc. Int. Conf. on Inorganic Scintillators and their Applications*, SCINT99, Russia, Moscow, 619, 2000.
- [79] A. Hofstaetter, M. V. Korzhik, V. V. Laguta, B. K. Meyer, V. Nagirnyi, and R. Novotny, “The role of defect states in the creation of intrinsic $(\text{WO}_4)^{3-}$ centers in PbWO_4 by sub-gap excitation”, *Rad. Measur.*, **33**, 533, 2001.
- [80] C. Itoh and S. Kigoshi, “Temperature dependence of the photocurrent excited above the fundamental absorption edge of PbWO_4 ”, *Phys. Stat. Sol. A*, **15**, 3774, 2006.

ACKNOWLEDGEMENTS

I have a great pleasure to thank people, who worked together with me, and the organizations, which contributed to the completion of this thesis.

First of all I wish to thank my brilliant supervisor Dr. Svetlana Zazubovich for initiating all these investigations, continuous support, help and advices. Working with her was useful, memorable and very pleasant experience.

I would like to express my words of acknowledgement to the Head of Laboratory of Physics of Ionic Crystals, Prof. Aleksandr Lushchik for possibility to carry out my research in this laboratory and for his continuous interest.

Next I report my deep acknowledgements to Dr. Mitsuru Ishii, Dr. Nachimuthu Senguttuvan from Shonan Institute of Technology, Fujisawa, Japan, Dr. Yoshiyuki Usuki from Furukawa Co., Ltd., Tsukuba, Japan and Dr. Pavel Bohachek from Institute of Physics, Czech Academy of Sciences, Prague, Czech Republic for preparation of the samples.

I am thankful to Dr. Vladimir Babin, Dr. Viktor Bichevin, Dr. Tiit Kärner, Dr. Tatiana Savikhina from the Laboratory of Physics of Ionic Crystals, Dr. Andres Stolovits from the Laboratory of Physics of Low Temperatures and Dr. Ilmo Sildos from the Laboratory of Laser Spectroscopy, for participating in and supporting for our joint investigations with their unique equipment, for scientific and technical help and a lot of ideas. I also wish to thank all the researchers from the Laboratory of Physics of Ionic Crystals, whose support, warm and friendly atmosphere and advices helped me a lot. Next, I would like to say words of acknowledgements to Dr. Aleksei Kotlov, Dr. Maksim Säkki, Dr. Sergey Shchemelyov, M.Sc. Andrei Kärkkänen, M.Sc. Aleksander Lissovski, M.Sc. Roman Tsubin, M.Sc. Veera Krasnenko and Vadim Boldenkov for being my friends and for help. I would also like to thank Dr. Sergei Dolgov and Dr. Valter Kiisk for technical help.

I would be glad to thank Dr. Martin Nikl from the Institute of Physics, Czech Academy of Sciences, Prague, Czech Republic for joint experiments, many useful advices, support, teaching and help. In addition, I would like to mention separately Dr. Eva Mihokova, Dr. Karel Polak and M.Sc. Natalia Solovieva.

I'm also grateful to Dr. Valentin Laguta from the Institute for Material Science, Ukrainian Academy of Sciences, Kiev, Ukraine for useful discussions and pleasant collaboration.

My very special thanks also to Dr. Gian Paolo Pazzi and Dr. Pasquale Fabeni from the Institute of Applied Physics, CNR, Florence, Italy for great and long-time collaboration.

I report my acknowledgements to Estonian Science Foundation for financial support during all these years.

I am thankful to North Atlantic Treaty Organization for possibilities to carry out scientific research with our colleagues from another countries and financial support.

I am also very thankful to my family for support and help.

PUBLICATIONS

E. Mihokova, M. Nikl, P. Bohacek, V. Babin, **A. Krasnikov**,
A. Stolovich, S. Zazubovich, A. Vedda, M. Martini, T. Grabowski,
“Decay kinetics of the green emission in $\text{PbWO}_4\text{:Mo}$ ”,
J. Lumin., vol. **102–103**, 618–622 (2003).

M. Nikl, P. Bohacek, E. Mihokova, V. Babin, A. Stolovitš, **A. Krasnikov**,
S. Zazubovich, G. P. Pazzi, P. Fabeni, A. Vedda, M. Martini,
“Excited state dynamics of luminescence centres in PbWO₄ single crystals”,
Functional Materials, vol. **10**, 105–110 (2003).

V. Babin, P. Bohacek, E. Bender, **A. Krasnikov**, E. Mihokova,
M. Nikl, N. Senguttuvan, A. Stolovits, Y. Usuki, S. Zazubovich,
“Decay kinetics of the green emission in tungstates and molybdates”,
Rad. Meas., vol. **38**, 533–537 (2004).

IV

P. Bohacek, N. Senguttuvan, V. Kiisk, **A. Krasnikov**, M. Nikl, I. Sildos,
Y. Usuki and S. Zazubovich, "Red emission of PbWO₄ crystals",
Rad. Meas., vol. **38**, 623–626 (2004).

P. Bohacek, P. Fabeni, **A. Krasnikov**, M. Nikl, G. P. Pazzi,
C. Susini, S. Zazubovich,
“Defects in UV-irradiated PbWO₄:Mo crystals monitored
by TSL measurements”, *Phys. Stat. Sol. (c)*, **2**, No.1, 547–550 (2005).

A. Krasnikov, M. Nikl, A. Stolovits, Y. Usuki, S. Zazubovich,
“Luminescence of the $\text{PbWO}_4:5\% \text{ Cd}$ crystal”,
Phys. Stat. Sol. (c) 2, No.1, 77–80 (2005).

P. Bohacek, P. Fabeni, **A. Krasnikov**, M. Nikl, G. P. Pazzi,
C. Susini, S. Zazubovich,
“Defects creation under UV irradiation of PbWO_4 crystals”,
Radiation Protection Dosimetry, **119**, No.1–4, 164–167 (2006).

VIII

A. Krasnikov, M. Nikl, S. Zazubovich,
“Localized excitons and defects in PbWO₄ single crystals:
a luminescence and photo-thermally stimulated disintegration study”
Phys. Stat. Sol. (b), **243**, No. 8, 1727–1743 (2006).

A. Krasnikov, M. Nikl, S. Zazubovich, “Processes resulting in thermal quenching of the blue emission in PbWO₄ crystals”, *Proceedings of the Eighth Int. Conf. on Inorganic Scintillators and Their Applications (SCINT'2005)*, Eds. A. Gektin, B. Grinyov (Alushta, Ukraine, 2006) p. 362–365.

P. Fabeni, V. Kiisk, **A. Krasnikov**, M. Nikl, G. P. Pazzi, I. Sildos,
and S. Zazubovich, “Tunneling recombination processes
in PbWO_4 ”, *Phys. Stat. Sol. (c)*, vol. **4**, pp. 918–921 (2007).

V. Babin, P. Bohachek, **A. Krasnikov**, M. Nikl, A. Stolovits,
S. Zazubovich “Origin of green luminescence in PbWO_4 crystals”,
J. Lumin., vol. **124**, 113–119 (2007).

P. Fabeni, **A. Krasnikov**, V. V. Laguta, M. Nikl, G. P. Pazzi, C. Susini,
and S. Zazubovich, “Origin of TSL peaks located at 200–250 K
in UV-irradiated PbWO₄ crystals”, *Rad. Measur.*, vol. **42**, 807–810 (2007).

A. Krasnikov, V. V. Laguta, M. Nikl, and S. Zazubovich,
“Localized excitons and their decay into electron and
hole centers in the PbWO_4 single crystals grown by
the Bridgman method”, *J. Phys.: Condens. Matter* 2007,
to be published.

CURRICULUM VITAE

Krasnikov Aleksei

Date and place of birth: May 6, 1977, Moscow, Russia
Citizenship: Estonian
Address: Institute of Physics, University of Tartu
Riia str. 142, 51014 Tartu, Estonia
Phone: +372 7 374 766
Fax: +372 7 383 033
E-mail: aleksei@fi.tartu.ee

Education

1984–1994 Tartu 6 Secondary School
2001 B.Sc. in physics, Faculty of Physics and Chemistry, University of Tartu
2003 M.Sc. in physics, Faculty of Physics and Chemistry, University of Tartu

Employment

2003–2007 University of Tartu, Ph.D. student (solid state physics)
2005–2007 Laboratory of Physics of Ionic Crystals, Institute of Physics, University of Tartu, engineer
2005–2007 Doctoral School of Material Science and Material Technologies, researcher.

Scientific work

Main field of research: solid state physics, scintillation materials, steady-state and time-resolved optical spectroscopy.
Total number of publications: 35

Awards

2004, 2005 – Estonian Education and Research Ministry, student award
2002 – Estonian Physical Society, student award

CURRICULUM VITAE

Krasnikov Aleksei

Sünniaeg ja -koht: 6. mai 1977. a. Moskva, Venemaa
Kodakondsus: Eesti
Aadress: Tartu Ülikooli Füüsika Instituut
Riia 142, 51014 Tartu, Eesti
Telefon: +372 7 374 766
Faks: +372 7 383 033
E-post: aleksei@fi.tartu.ee

Hariduskäik

1984–1994 Tartu 6. Keskkool (füüsika ja matemaatika haru)
2001 B.Sc. füüsikas, Tartu Ülikooli füüsika-keemiateaduskond
2003 M.Sc. füüsikas, Tartu Ülikooli füüsika-keemiateaduskond

Teenistuskäik

2003–2007 Tartu Ülikool, doktorant
2005–2007 Tartu Ülikooli Füüsika Instituudi ioonkristallide labor, insener
2005–2006 Tartu Ülikooli Materjaliteaduse ja Materjalide Tehnoloogia
Doktrikool, erakorraline teadur

Teadustegevus

Peamine töösuund: tahke keha füüsika, stsintillatsioonmaterjalid, statsionaarne ja aeglahutusega optiline spektroskoopia.
Publikatsioone: 35

Teaduspremiad

2004, 2005 – Haridus- ja Teadusministeerium, üliõpilaspreamia
2002 – Eesti Füüsika Selts, üliõpilaspreamia

DISSERTATIONES PHYSICAE UNIVERSITATIS TARTUENSIS

1. **Andrus Ausmees.** XUV-induced electron emission and electron-phonon interaction in alkali halides. Tartu, 1991.
2. **Heiki Sõnajalg.** Shaping and recalling of light pulses by optical elements based on spectral hole burning. Tartu, 1991.
3. **Sergei Savihhin.** Ultrafast dynamics of F-centers and bound excitons from picosecond spectroscopy data. Tartu, 1991.
4. **Ergo Nõmmiste.** Leelishalogeniidide röntgenelektronemissioon kiiritamisel footonitega energiaga 70–140 eV. Tartu, 1991.
5. **Margus Rätsep.** Spectral gratings and their relaxation in some low-temperature impurity-doped glasses and crystals. Tartu, 1991.
6. **Tõnu Pullerits.** Primary energy transfer in photosynthesis. Model calculations. Tartu, 1991.
7. **Olev Saks.** Attoampri diapsoonis voolude mõõtmise füüsikalised alused. Tartu, 1991.
8. **Andres Virro.** AlGaAsSb/GaSb heterostructure injection lasers. Tartu, 1991.
9. **Hans Korge.** Investigation of negative point discharge in pure nitrogen at atmospheric pressure. Tartu, 1992.
10. **Jüri Maksimov.** Nonlinear generation of laser VUV radiation for high-resolution spectroscopy. Tartu, 1992.
11. **Mark Aizengendler.** Photostimulated transformation of aggregate defects and spectral hole burning in a neutron-irradiated sapphire. Tartu, 1992.
12. **Hele Siimon.** Atomic layer molecular beam epitaxy of A^2B^6 compounds described on the basis of kinetic equations model. Tartu, 1992.
13. **Tõnu Reinot.** The kinetics of polariton luminescence, energy transfer and relaxation in anthracene. Tartu, 1992.
14. **Toomas Rõõm.** Paramagnetic H^{2-} and F^+ centers in CaO crystals: spectra, relaxation and recombination luminescence. Tallinn, 1993.
15. **Erko Jalviste.** Laser spectroscopy of some jet-cooled organic molecules. Tartu, 1993.
16. **Alvo Aabloo.** Studies of crystalline celluloses using potential energy calculations. Tartu, 1994.
17. **Peeter Paris.** Initiation of corona pulses. Tartu, 1994.
18. **Павел Рубин.** Локальные дефектные состояния в CuO_2 плоскостях высокотемпературных сверхпроводников. Тарту, 1994.
19. **Olavi Ollikainen.** Applications of persistent spectral hole burning in ultrafast optical neural networks, time-resolved spectroscopy and holographic interferometry. Tartu, 1996.
20. **Ülo Mets.** Methodological aspects of fluorescence correlation spectroscopy. Tartu, 1996.

21. **Mikhail Danilkin.** Interaction of intrinsic and impurity defects in CaS:Eu luminophors. Tartu, 1997.
22. **Ирина Кудрявцева.** Создание и стабилизация дефектов в кристаллах KBr, KCl, RbCl при облучении ВУФ-радиацией. Тарту, 1997.
23. **Andres Osvet.** Photochromic properties of radiation-induced defects in diamond. Tartu, 1998.
24. **Jüri Örd.** Classical and quantum aspects of geodesic multiplication. Tartu, 1998.
25. **Priit Sarv.** High resolution solid-state NMR studies of zeolites. Tartu, 1998.
26. **Сергей Долгов.** Электронные возбуждения и дефектообразование в некоторых оксидах металлов. Тарту, 1998.
27. **Кауро Кукли.** Atomic layer deposition of artificially structured dielectric materials. Tartu, 1999.
28. **Ivo Heinmaa.** Nuclear resonance studies of local structure in $\text{RbBa}_2\text{Cu}_3\text{O}_{6+x}$ compounds. Tartu, 1999.
29. **Aleksander Shelkan.** Hole states in CuO_2 planes of high temperature superconducting materials. Tartu, 1999.
30. **Dmitri Nevedrov.** Nonlinear effects in quantum lattices. Tartu, 1999.
31. **Rein Ruus.** Collapse of 3d (4f) orbitals in 2p (3d) excited configurations and its effect on the x-ray and electron spectra. Tartu, 1999.
32. **Valter Zazubovich.** Local relaxation in incommensurate and glassy solids studied by Spectral Hole Burning. Tartu, 1999.
33. **Indrek Reimand.** Picosecond dynamics of optical excitations in GaAs and other excitonic systems. Tartu, 2000.
34. **Vladimir Babin.** Spectroscopy of exciton states in some halide macro- and nanocrystals. Tartu, 2001.
35. **Toomas Plank.** Positive corona at combined DC and AC voltage. Tartu, 2001.
36. **Kristjan Leiger.** Pressure-induced effects in inhomogeneous spectra of doped solids. Tartu, 2002.
37. **Helle Kaasik.** Nonperturbative theory of multiphonon vibrational relaxation and nonradiative transitions. Tartu, 2002.
38. **Tõnu Laas.** Propagation of waves in curved spacetimes. Tartu, 2002.
39. **Rünno Lõhmus.** Application of novel hybrid methods in SPM studies of nanostructural materials. Tartu, 2002.
40. **Kaido Reivelt.** Optical implementation of propagation-invariant pulsed free-space wave fields. Tartu, 2003.
41. **Heiki Kasemägi.** The effect of nanoparticle additives on lithium-ion mobility in a polymer electrolyte. Tartu, 2003.
42. **Villu Repän.** Low current mode of negative corona. Tartu, 2004.
43. **Алексей Котлов.** Оксианионные диэлектрические кристаллы: зонная структура и электронные возбуждения. Tartu, 2004.

44. **Jaak Talts.** Continuous non-invasive blood pressure measurement: comparative and methodological studies of the differential servo-oscillometric method. Tartu, 2004.
45. **Margus Saal.** Studies of pre-big bang and braneworld cosmology. Tartu, 2004.
46. **Eduard Gerškevičš.** Dose to bone marrow and leukaemia risk in external beam radiotherapy of prostate cancer. Tartu, 2005.
47. **Sergey Shchemelyov.** Sum-frequency generation and multiphoton ionization in xenon under excitation by conical laser beams. Tartu, 2006.
48. **Valter Kiisk.** Optical investigation of metal-oxide thin films. Tartu, 2006.
49. **Jaan Aarik.** Atomic layer deposition of titanium, zirconium and hafnium dioxides: growth mechanisms and properties of thin films. Tartu, 2007.
50. **Astrid Rekker.** Colored-noise-controlled anomalous transport and phase transitions in complex systems. Tartu, 2007.
51. **Andres Punning.** Electromechanical characterization of ionic polymer-metal composite sensing actuators. Tartu, 2007.
52. **Indrek Jõgi.** Conduction mechanisms in thin atomic layer deposited films containing TiO₂. Tartu, 2007.